Identification of a Robust Antibody Modulator of CD33 in In Vitro Models

Identification of a Robust Antibody Modulator of CD33 in *In Vitro* Models

Arica Aiello

A Thesis in the Field of Biology

for the Degree of Master of Liberal Arts in Extension Studies

Harvard University

November 2023

Abstract

CD33 is a sialic acid binding immunoglobulin-type lectin found on myeloid cells throughout the body, including microglia, the brain's resident immune cells. CD33 has been implicated genetically in late-onset Alzheimer's disease (LOAD) as both a potential risk factor and potential protective factor. This is based on the alternative splicing of CD33, which produces two isoforms of the protein: a full-length isoform, and a shorter isoform lacking the extracellular sialic acid binding domain. Because of its implication in disease, CD33 may be a potential therapeutic target for AD. A previous study by Wißfeld, et al. (2021) has designed a reporter cell assay capable of monitoring CD33 activation. Using this model, we were able to identify a robust antibody modulator of CD33, rabbit monoclonal E6V7H. Endogenous models expressing CD33, THP-1 and TF-1, were also tested using E6V7H for CD33 activation. We found that treating these cells with E6V7H altered the expression levels of downstream phospho-SHP-1, but more work needs to be done on the downstream signaling of CD33 to create an endogenous readout of CD33 activation.

Dedication

This thesis is dedicated to my loving partner, Joe. Thank you for your love and support throughout this process. Thank you for keeping me on track and taking care of things when I spent my weekends in the lab. I couldn't have done it without you.

Acknowledgments

Thorsten Wiederhold, Ph.D.—My thesis director, who acted as both a mentor and support system throughout this process. The biggest thank you for everything.

Richard Cho, Ph.D.—My manager at work, who's full support of this work allowed me to accomplish this goal this year.

Melissa Romaneck—A trusted friend and colleague who helped guide my thought process and keep me grounded throughout the process.

Angela Merluzzo—A trusted colleague and tissue culture expert who enthusiastically helped me establish a "home base" in the tissue culture room and provided protocols and help along the way. Thank you for your expertise and kindness throughout this process!

Kayley LeFrancois and Alison Cocchiola — Thank you both for all the help you provided in assisting with generating my stable cell lines, supplying buffers, and liquid nitrogen storage for my cell lines.

The Western blot core at Cell Signaling Technology, Inc. graciously allowed me to use their bench space and buffers throughout the process.

Table of Contents

List of Tables

List of Figures

Chapter I.

Introduction

This chapter introduces the key concepts, background information, and research aims involved in crafting this thesis.

Alzheimer's Disease, a Public Health Crisis

Alzheimer's disease (AD) is a slowly progressive neurodegenerative disease and the most common form of dementia worldwide, characterized by physiological biomarkers and patient cognitive decline. As AD progresses, the disease destroys the patient's memory, cognitive skills, and ultimately their ability to carry out basic functions. The number of AD cases is increasing as the aging population increases, with numbers expected to reach 152 million patients by 2050. Along with the burden on patients and their families, there is a growing burden on the healthcare system, with expected global costs reaching one trillion US dollars per year (Breijyeh & Karaman, 2020). Increased investments have been made toward AD research and drug development with very low success rates seen in attempted drug therapies. Key factors that likely play a role in low success rates include gaps in knowledge of late onset AD (LOAD), lack of patients within early disease stages, and potentially incorrect therapeutic targeting (Gauthier et al., 2016; Cummings et al., 2014; Macklin, 2021). Recently, two monoclonal antibodies targeting β-amyloid have been approved for treatment of AD and have been shown to slow the progression of the disease (Cummings, 2023). While this therapy is a huge breakthrough in treatment options, there is currently no cure for AD and further

research into fully understanding the underlying disease mechanisms is critical to improving this growing public health crisis.

Alzheimer's Disease Pathology

AD is currently characterized by two main pathological hallmarks; intracellular tau neurofibrillary tangles (NFTs) and extracellular β-amyloid (Aβ) plaques, ultimately leading to reduced synaptic strength, synaptic loss, and neurodegeneration. β-amyloid plaques are formed through the processing of amyloid precursor protein (APP). APP processing occurs through cleavage by β-secretase and γ-secretase forming Aβ peptide fragments. The two major isoforms of Aβ peptide formed through APP processing are Aβ42 and Aβ40, named for their sequence residue numbers. Although Aβ40 is the more abundant fragment, Aβ42 has been shown to form the major component of amyloid plaques in AD (Gu & Guo, 2013).

Other alterations contributing to AD are metabolic, vascular, and inflammatory changes that affect disease progression (Lopez et al., 2019; Yamazaki et al., 2019; Knopman et al., 2021). In more recent years, a strong focus has shifted to the inflammatory changes that occur in AD and how they impact disease onset and progression. Neuroinflammatory markers have been reported in both human AD patients (Shen et al., 2019) and in animal models of the disease (Schwab et al., 2010). These inflammatory changes appear to be initially neuroprotective, activating immune cells to remove and clear the potential threat. However, issues arise when this activation becomes chronic, as neuroinflammation appears to increase Aβ plaque and tau NFT burden in AD (Kinney et al., 2018).

Microglia, the brain's resident immune cells, have been implicated in both protection against AD and exacerbation of disease. Under normal conditions, microglia remain in an inactive state, surveying their environment and communicating with neurons and glia. In response to a potential threat, microglia are activated, leading to release of pro-inflammatory molecules such as reactive oxygen species, nitric oxide, and cytokines like IL-1 and IL-6 (Kinney et al., 2018; Wang et al., 2015; Lajaunias et al., 2005). Microglia also undergo morphological changes that lead to cell enlargement, process retraction, and migration. A key function of microglia is maintaining tissue homeostasis through phagocytosis of debris. In AD, it is hypothesized that Aβ peptides may be the main driver of microglial activation, as activated microglia migrate to and surround Aβ plaques (Kinney et al., 2018). Studies have shown that microglia phagocytose Aβ and are successful at clearing Aβ and delaying disease progression in mouse models of AD (Hickman et al., 2008). However, persistent Aβ accumulation leading to prolonged microglial activation has a deleterious effect on the ability of microglia to continue to phagocytose and clear Aβ, leading to further accumulation of plaques. This prolonged microglial activation also leads to sustained proinflammatory cytokine signaling, which downregulates genes involved in microglial Aβ clearance, thus exacerbating the plaque burden and damaging neurons (Hickman et al., 2008). Several genome wide association studies (GWAS) have implicated microglial genes in late-onset Alzheimer's disease (LOAD), including myeloid cell receptor CD33, TREM2, ABCA7, and INPP5D/SHIP1 (Naj et al., 2011; Efthymiou & Goate, 2017).

Siglec Proteins

Sialic-acid binding immunoglobulin-like lectins, or Siglecs, are a family of type I transmembrane proteins mainly expressed on immune cells. There are two subsets of Siglec proteins, one group conserved across mammals, and the other that is variable in mammals called CD33-related Siglecs. The majority of Siglec proteins contain tyrosine-based signaling motifs, specifically tyrosine-based inhibitory motifs (ITIMs). The CD33-related Siglecs mostly have two ITIM motifs, important for the recruitment of SRC homology 2 (SH2)-domain-containing protein tyrosine phosphatases. Siglec proteins also contain a V-set immunoglobulin domain capable of binding sialic acids (Figure 1). These sialic acids can be expressed by pathogens, leading to an alteration of immune response by the Siglec proteins. Depending on the pathogen, this alteration of immune response may be beneficial or detrimental to the host. For example, Siglec-dependent uptake could promote pathogen destruction and antigen presentation. On the other hand, the CD33-related Siglecs may inhibit the immune response through ITIM-mediated signaling (Crocker et al., 2007).

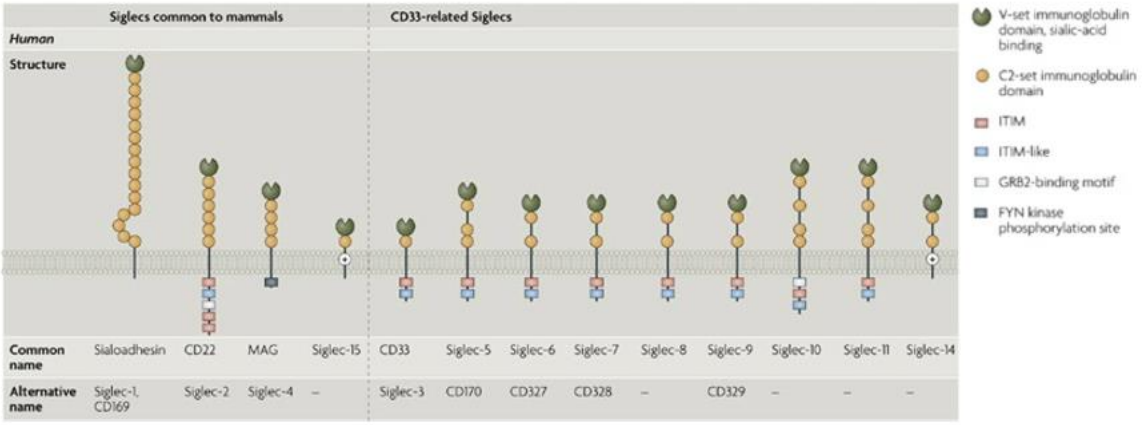

Figure 1: The structure and domains of major Siglec proteins

This figure from Crocker et al. (2007) showcases the structure and domains of major human Siglec protein family members. Siglec proteins are type I transmembrane proteins characterized by their extracellular amino terminal V-set immunoglobulin (sialic acid binding) domain and varying number of C2-set immunoglobulin domains. The CD33-related Siglecs contain two intracellular ITIM domains on their C-terminus (Crocker et al., 2007).

CD33 (Siglec-3)

Cluster of differentiation 3 (CD33), also called Siglec-3, is a type I transmembrane protein member of the previously described sialic acid-binding immunoglobulin-like lectin family expressed on myeloid immune cells throughout the body. CD33 has many functions within the immune system including participation in immune cell adhesion and interaction with sialyated pathogens, likely facilitating endocytosis by phagocytes (Jiang et al., 2014). CD33 is also known to be responsible for mediating inhibitory signaling of immune cells, affecting normal functions like phagocytosis, apoptosis, and cytokine release (Zhao, 2018). In the brain, CD33 is expressed on microglia and infiltrating macrophages and has been shown to modulate microglial activation (Zhao, 2018; Crocker et al., 2007).

CD33 contains two extracellular domains on its amino-terminus, including a variable (V)-type Ig-like domain responsible for sialic acid binding, and a C2-type Ig-like domain. The V-type Ig-like domain is located within amino acid sequence 19-135 of human CD33, while the C2-type Ig-like domain is within amino acid sequence 145-228 (Zhao, 2018) (Figure 2, A; Jiang et al., 2014). It has been strongly suggested that amino acid R119, a highly conserved site among family members, is the critical residue responsible for functional sialic acid binding (Miles et al., 2019).

Intracellularly, CD33 contains two ITIM motifs that, when phosphorylated, act as a docking site for recruitment and activation of tyrosine phosphatases. Within these recruited proteins are those that contain a Src homology (SH) 2 domain (SH2), like SHP phosphatases (Zhao, 2018). Studies have shown that SHP-1 and SHP-2 specifically bind to CD33's ITIM domain leading to downstream immune inhibitory affects (Paul et al., 2000; Taylor et al., 1999). Upon CD33 activation, SHP-1 and SHP-2 are recruited through phosphorylation on key activating sites, such as Y564 on SHP-1 and Y542 on SHP-2 (Abram & Lowell, 2017; Lu et al., 2001). This initial recruitment and activation increases the protein's phosphatase activity leading to downstream dephosphorylation of proteins like PI3 kinase or spleen tyrosine kinase (SYK), that lead to inhibition of key cellular processes like phagocytosis (Estus et al., 2019; Jonas et al., 2022).

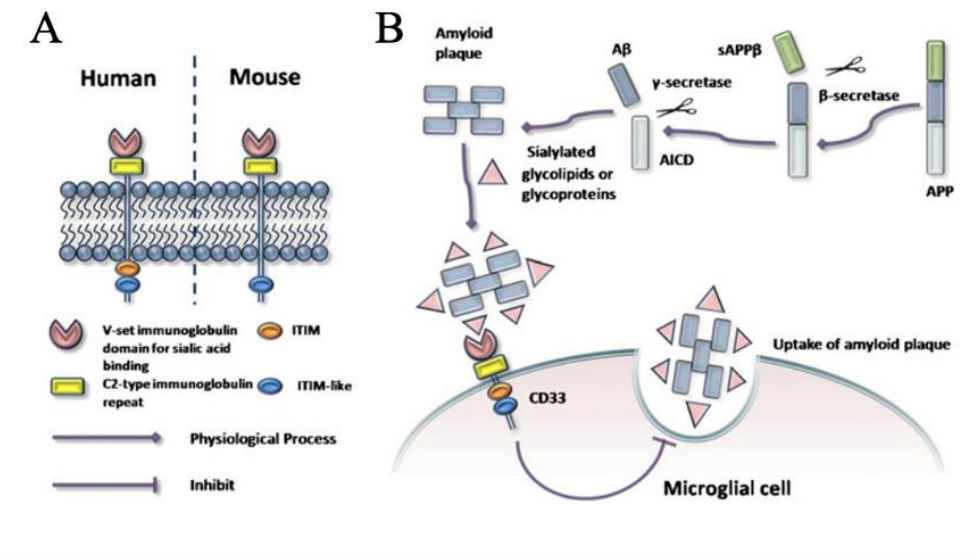

Figure 2: CD33 structure, domains, and role in inhibiting A clearance through Aβ clearance through binding sialylated Aβ

This figure from Jiang et al. (2014) shows the structure and subcellular location of human CD33, highlighting the extracellular V-set immunoglobulin domain for sialic acid binding, C2-type immunoglobulin repeat domain, and the ITIM and ITIM-like domains on the intracellular C-terminus (A). This figure also highlights the possible mechanism for CD33's implication in impairing microglial clearance of Aβ. Aβ peptides become sialylated, binding to the extracellular V-set immunoglobulin domain of CD33, activating the protein's inhibitory pathway, thus, blocking normal microglial uptake of Aβ (Jiang et al., 2014).

CD33 and Alzheimer's Disease

Genome wide association studies (GWAS) have identified several polymorphisms associated with LOAD in genes expressed by microglia, including CD33 (Naj et al., 2011). CD33 single nucleotide polymorphisms (SNPs) identified by GWAS have been implicated in both LOAD pathology, susceptibility, and protection. The most common allele associated with LOAD is rs3865444C, which is implicated to increase risk of LOAD and is linked to more severe cognitive decline. Conversely, a second and rarer

allele, rs3865444A, may confer protection against LOAD. It is thought that this is due to modulation of overall CD33 expression and the splicing of exon 2, responsible for coding CD33's sialic acid binding domain, that leads to truncated (D2-CD33, ΔE2-CD33) or full-length (CD33M) isoforms of CD33. However, due to its location, rs3865444 is not likely to affect exon 2 splicing. Another SNP, in linkage disequilibrium with rs3865444, is rs12459419, which is located within exon 2. Further investigation shows that allele rs12459419T is co-inherited with rs3865444A and together increase the chance of exon 2 skipping, leading to increased expression of D2-CD33 and decreased expression of CD33M, ultimately conferring protection against LOAD (Zhao, 2018; Bhattacherjee et al., 2021).

The difference between the truncated D2-CD33 isoform and the full-length CD33M isoform is the lack of sialic acid binding domain in the D2-CD33 isoform. This prevents activation of CD33 and prevent its inhibitory effect on phagocytic cells, like microglia. Figure 3 shows a possible signaling pathway of CD33M activation compared to the D2-CD33 isoform. It has been shown that the T allele of SNP rs3865444 is also corelated with lower brain CD33 expression in microglia and lower levels of insoluble Aβ42, showing that lowering CD33 levels may also play an important role in protection against LOAD (Griciuc et al., 2013). This information infers that CD33 has an inhibitory effect on microglial ability to phagocytose and clear toxic Aβ peptides, illustrated by Jiang, et al. (Figure 2, B). Griciuc et al. (2013) have shown that in transgenic mouse models of AD displaying amyloid-plaque pathology, knockout of CD33 markedly reduced insoluble Aβ42 levels and decreased overall amyloid plaque burden (Griciuc et al., 2013). Another study generated a transgenic mouse whose microglial cell lineage

expressed the D2-CD33 isoform of CD33 and showed that the efficiency of microglial phagocytosis was increased, suggesting that the D2-CD33 isoform may provide a gain of function (Bhattacherjee et al., 2021).

Another gene implicated in LOAD GWAS, TREM2, has been shown to act downstream of CD33 in an opposing manner (Griciuc et al., 2019). The TREM2 mutation associated with AD reduces ligand binding and impairs microglial phagocytosis of Aβ, where D2-CD33 prevents ligand interaction through its sialic acid binding domain leading to decreased inhibitory function through ITIM signaling, increasing Aβ phagocytosis (Hansen et al., 2018). There is a delicate balance of microglial activation within AD, where maintaining phagocytosis of debris, like Aβ, decreases its neurotoxic affects but may lead to a change in microglial phenotype, affecting the ability to continue appropriate phagocytic clearance (Wang et al., 2015). While further investigation is needed, this information together infers that CD33 may be a therapeutic target for AD to appropriately promote the clearance of toxic Aβ species.

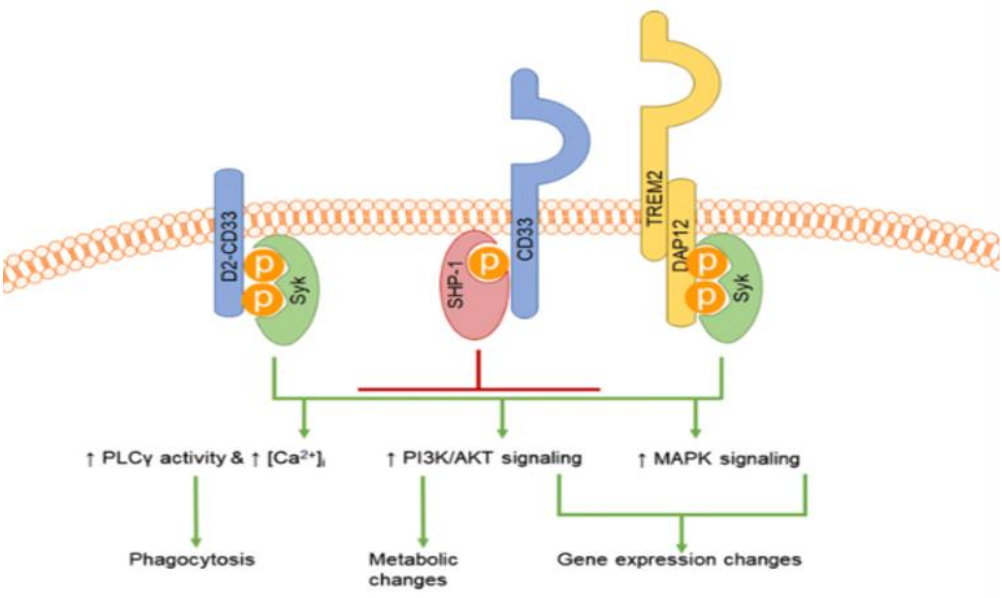

Figure 3: CD33M and D2-CD33 signaling diagram

A diagram from Estus et al.(2019) showing the downstream signaling pathway for both CD33M and D2-CD33. Activation of CD33M recruits SHP phosphatases, like SHP-1 that bind to the intracellular ITIM domain of CD33, blocking SYK recruitment and phosphorylation, leading to inhibitory immune affects. The D2-CD33 isoform lacking the extracellular sialic acid binding domain blocks CD33 activation and allows for downstream activation of the TREM2 pathway, recruiting DAP12 and SYK phosphorylation, leading to increase in immune response like phagocytosis (Estus et al., 2019).

CD33 Reporter Cell Assay

Wißfeld et al. (2021) previously published a reporter cell line that can be used to investigate ligands and antibodies capable of modulating CD33 signaling. They validated this model on specific CD33 activating antibodies and on human iPSC-derived microglia. The reporter cell line was created by expressing a fusion protein containing the extracellular domain of CD33, containing the sialic acid binding domain, with TYRO protein tyrosine kinase binding protein (TYROBP), also known as DAP12, linked to the

intracellular portion of the construct. They also generated a version of this fusion protein to mimic the Alzheimer's disease protective variant CD33ΔE2, which lacks the sialic acid binding domain (Figure 4, A). They show that they can modulate CD33 activation through treatment of the cell lines with CD33 antibodies mapped to the extracellular region of CD33. Using the DAP12 linker, they show that phospho-SYK can be used as a readout of this CD33 modulation, as SYK phosphorylation events occur downstream of DAP12 (Figure 4, B). To prevent TREM2 interaction, their construct was modulated with a point mutation of a key amino acid on the DAP12 gene, D50A. They also show that the phospho-SYK readout is present in the CD33-DAP12 cells but not present in the CD33ΔE-DAP12 cells, making this a strong model for identifying antibody-based modulators of CD33. Based on this reporter cell assay, Wißfeld et al. (2021) have shown that two CD33 mouse monoclonal antibody clones can modulate CD33 activity; 1c7/1 and P67.6. Wißfeld et al. (2021) also mapped the epitopes of both 1c7/1 and P67.6. They determined that 1c7/1 binds an epitope within the C2-set Ig-like domain, because it can detect both CD33 constructs. The P67.6 antibody was mapped to the V-type Ig-like because it can only detect the CD33-DAP12 construct. These two antibodies were utilized as positive controls when identifying other antibody modulators of CD33.

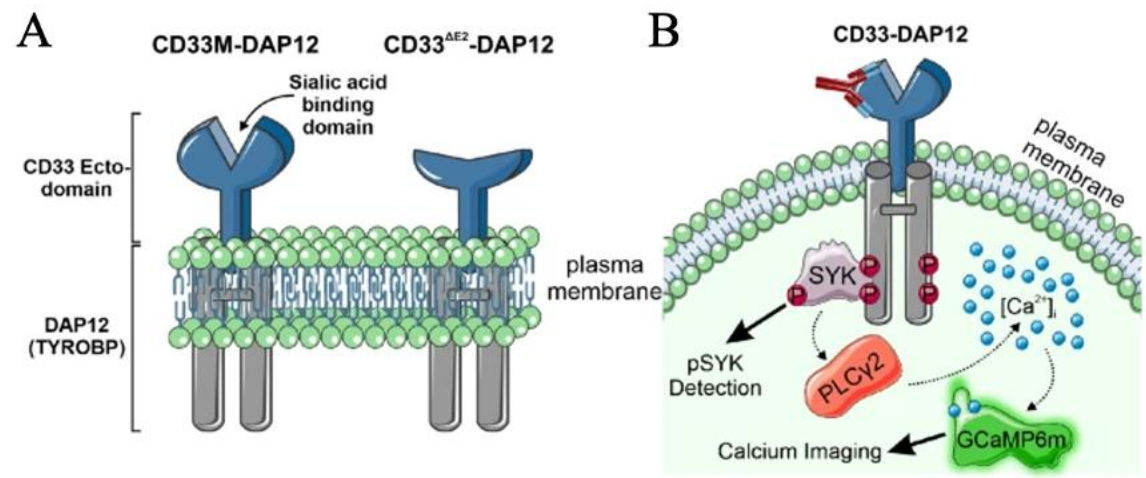

Figure 4: A visual diagram of Wißfeld et al. (2021) reporter cell assay plasmids and readout

Wißfeld et al. (2021) showcase the subcellular location and structure of their established fusion protein containing the full ecto-domain of CD33 linked to DAP12 on the intracellular portion of the construct (A, left). The ΔE2-CD33 variation is also shown with a disruption in the sialic acid binding domain, still linked to DAP12 on the intracellular portion of the construct (A, right). A diagram of the reporter cell assay is provided (B) showing antibody binding to the sialic acid binding domain, increasing phosphorylation of SYK through DAP12 as a downstream readout of CD33 activation (Wißfeld et al., 2021)

Definition of Terms

Alzheimer's Disease (AD): A genetic and sporadic neurodegenerative disease biologically defined by β-amyloid plaques and tau neurofibrillary tangles and neuronal cell death leading to cognitive impairment (Knopman et al., 2021).

Beta-Amyloid (Aβ) plaque: An extracellular accumulation of amyloid-beta peptide cleavage products of amyloid precursor protein (Knopman et al., 2021).

CD33: Cluster of differentiation 33 (CD33), also known as sialic acid-binding immunoglobulin-like lectin 3 (Siglec-3) is a myeloid receptor expressed by microglia and macrophages in the brain. CD33 is an Alzheimer's disease risk factor identified by genome wide association studies (Zhao, 2019).

CD33M or WT-CD33: The full-length isoform of CD33 with all known domains intact.

D2-CD33 or ΔE2-CD33: Domain 2-CD33 or ΔE2 (change in exon 2) is the truncated isoform of CD33 where the IgV ligand binding domain, or sialic acid binding domain, is removed from the sequence (Wißfeld et al., 2021).

Genome Wide Association Study (GWAS): GWAS are studies where genetic variants are identified across many individuals to investigate genotype to phenotype relationships. GWAS are helpful in identifying key genetic variations in disease phenotypes (Tam et al., 2019).

HMC-3: Human microglial clone 3 cell line is an immortalized cell line established through SV40-dependent immortalization of human embryonic microglial cells (Russo et al., 2018).

ITIM domain: The immunotyrosine inhibitory motif (ITIM) is a domain involved in inhibitory signal transduction in cells (Zhao, 2018).

Late-onset Alzheimer's disease (LOAD): Late-onset Alzheimer's disease is the most common form of AD, where symptoms begin at age 65 or later. LOAD can be caused sporadically, by genetics, or environmentally (Rabinovici, 2019).

Linkage disequilibrium: Linkage disequilibrium is the nonrandom association of alleles at two or more loci (Slatkin, 2008).

Neurodegeneration: Neurodegeneration is the slow progressive loss of neurons associated with diseases like Alzheimer's disease (Gao & Hong, 2018).

Neurofibrillary tangle (NFT): Intracellular accumulation of tau protein that forms neurofibrillary tangles within neurons and leads to Alzheimer's disease pathology (Knopman et al., 2021).

rs12459419C: One of the SNPs identified in GWAS of Alzheimer's disease. This allele correlates with increased susceptibility of Alzheimer's disease (Bhattacherjee et al., 2021).

rs12459419T: One of the SNPs identified in GWAS of Alzheimer's disease. This allele correlates with decreased susceptibility of Alzheimer's disease and skipping of exon 2 (Bhattacherjee et al., 2021).

rs3865444A: One of the SNPs identified in GWAS of Alzheimer's disease. This allele is located on exon two and in linkage disequilibrium with rs12459419T (Bhattacherjee et al., 2021).

Single nucleotide polymorphism (SNP): A single nucleotide polymorphism is a variation in a gene by one single base pair. SNPs are used in GWAS to identify associations with genetic variation and disease states (Tam et al., 2019).

Research Aims

The primary research goal of this thesis was to identify a robust *in vitro* activator of the CD33 signaling pathway to promote further investigation and targeting of previously identified AD risk factor, CD33, as a potential therapeutic target. Based on the literature, mouse monoclonal antibodies toward the sialic acid binding V-set domain have been identified as potential modulators of CD33, however, rabbit monoclonal antibodies have strong advantages over mouse antibodies in target specificity and affinity (Weber et

al., 2017). This thesis will confirm previously established results, aims to add to this antibody portfolio by identifying a rabbit monoclonal antibody capable of activating CD33, and will investigate the ability of these antibodies to activate the CD33 pathway endogenously.

Aim 1 of this study was to replicate the CD33 cell reporter assay and results established by Wißfeld et al. (2021). To do this, plasmids for both CD33-DAP12 and CD33ΔE-DAP12 were designed, synthesized, sequenced, and expression was confirmed by Western blot. From here, stable transfection conditions were optimized, and stable transfection cell lines were generated for both plasmids. Two identified CD33 activating mouse monoclonal antibodies were used to treat the cells and the phospho-SYK readout was confirmed by ELISA.

Aim 2 of this study was to identify a robust modulator of CD33 *in vitro* by testing multiple rabbit host antibodies with varying epitopes on a previously established CD33 reporter cell assay. A rabbit monoclonal antibody, E6V7H, was confirmed to activate CD33 based on the reporter cell assay.

Aim 3 of this study was to utilize an immortalized human microglia cell line (HMC3) to introduce WT-CD33 and ΔE2-CD33 and attempt to activate the pathway using the newly established CD33 activating antibody, E6V7H.

Aim 4 of this study was to validate the identified CD33 activating antibody (E6V7H) on endogenous *in vitro* cell models of CD33. Cell lines THP-1 and TF-1 were confirmed to express endogenous levels of CD33. These cell lines were treated with E6V7H and downstream signaling targets were tested to determine change in protein levels upon CD33 stimulation with E6V7H.

Chapter II.

Materials and Methods

This chapter describes the materials and methods used throughout this thesis looking at CD33 activation in a reporter cell assay and endogenous models.

Cell Culture

HEK/293 cells (CRL-1573, ATCC) and HMC3 cells (CRL-3304, ATCC) were cultured according to an adapted version of the manufacturer's guidelines. Frozen cells were thawed quickly in pre-warmed media (Minimum Essential Medium, 10% fetal bovine serum (FBS), 1% sodium pyruvate, 1X non-essential amino acids, 100 I.U./mL penicillin and 100 µg/mL streptomycin). The cells were passaged upon reaching 80-90% confluency by removing media, washing the plate with sterile 1X phosphate buffered saline (PBS), and detaching the cells chemically using 0.25% Trypsin-ethylenediaminetetraacetic acid (EDTA) (25200056, ThermoFisher Scientific). Cells were incubated at 37°C with 5% CO.

THP-1 cells (TIB-202, ATCC) and TF-1 cells (CRL-2003, ATCC) were cultured according to an adapted version of the manufacturer's guidelines. Frozen cells were thawed quickly in pre-warmed media (RPMI-1640 Medium, 10% fetal bovine serum (FBS), 1% sodium pyruvate, 100 I.U./mL penicillin and 100 µg/mL streptomycin). TF-1 cells were supplemented with recombinant human GM-CSF (#87015, Cell Signaling Technology, Inc.) at a concentration of 2 ng/mL. The cells were passaged upon reaching

70% confluency by removing media, spinning cells down in a centrifuge, washing cells with sterile 1X PBS, and seeding them into new plates supplemented with fresh media. Cells were incubated at 37°C with 5% CO. A list of cell lines used can be found in Table 1.

Transfection Protocol and Optimization

All plasmids, listed in Table 2, were validated in HEK/293 cells using an optimized version of the Lipofectamine manufacturer's transfection protocol. The transfection protocols were then optimized to suit HEK/293 cell transfection and HMC3 transfection. 24 hours prior to transfection, HEK/293 cells were seeded at a density of 1x105 cells/mL and HMC3 cells were seeded at a density of 2x105 cells/mL in pre-warmed antibiotic free media (Minimum Essential Medium, 10% fetal bovine serum (FBS), 1% sodium pyruvate, 1X non-essential amino acids). Prior to transfection, cell media was changed to serum free/antibiotic free Minimum Essential Medium. Either 2, 4, or 6 μg of DNA were incubated for 5 minutes in serum free/antibiotic free Minimum Essential Medium. Lipofectamine 2000 (11668-500, LifeTechnologies) was incubated for 5 minutes in serum free/antibiotic free Minimum Essential Medium at a ratio of 1:5 DNA to Lipofectamine. The DNA and Lipofectamine mixtures were then combined, mixed gently, and allowed to incubate for 5 minutes at room temperature. The Lipofectamine/DNA mixtures were then added dropwise to their appropriate cell culture plate. The plates were swirled to mix and ensure even distribution of the transfection.

Geneticin/G418 Dose Response Curve

A dose response curve was generated for each HEK/293 and HMC3 cell lines to determine the optimal concentration of Geneticin/G418 antibiotic for selecting stable cell colonies. Cells were plated in two 6-well tissue culture plates until approximately 80% confluence. Increasing amounts of Geneticin/G418 were added to the media at concentrations of 0, 50, 100, 200, 300, 400, 500, 600, 700, 800, 900, and 1000 µg/mL. The cells were examined every day for seven days with visual toxicity and confluence measured for HEK/293 and HMC3. Media and cell debris were removed, and media replenished, reintroducing Geneticin/G418 every three days for up to one week.

Generation of the 293/CD33-DAP12 and 293/ΔE2CD33-DAP12 Stable Transfection Cell Lines

HEK-293 cells were cultured, as previously described, in 6-well tissue culture plates at 70% confluence. Media was replaced with serum-free and antibiotic free Opti-MEM™ Reduced Serum Medium (ThermoFisher Scientific) supplemented with 1% sodium pyruvate and 1X non-essential amino acids. Transfections were performed as described previously using Lipofectamine 2000 and previously optimized 2 µg of construct DNA (Table 2). Transfections were incubated for 6 hours at 37°C. After the incubation period, filtered Opti-MEM™+20% FBS was added to each well up to a final 10% FBS concentration. Transfections were then incubated again at 37°C for 24 or 48 hours. After the transfection period, media was removed from each well and replaced with selection media. For HEK/293 cells the selection media was composed of Opti-MEM™+10% FBS, 1% sodium pyruvate, 1X non-essential amino acids, 100 I.U./mL penicillin and 100 µg/mL streptomycin, and 900 µg/mL of Geneticin/G418. For the

HMC3 cells the selection media Opti-MEM™+10% FBS, 1% sodium pyruvate, 1X non-essential amino acids, 100 I.U./mL penicillin and 100 µg/mL streptomycin, and 1000 µg/ml of Geneticin/G418. The selection media was changed every 2-3 days to ensure proper cell health and to clear debris from cell death. After the selection process, the cells were expanded into single cell colonies in a 96-well plate. Strong single colony clones were then expanded into 6-well tissue culture plates. Once cells reached up to 80% confluence, cells were then split evenly between a 10 cm tissue culture plate for continued use and a 6-well plate for Western blot validation.

Culture of 293/CD33-DAP12 and 293/ΔE2CD33-DAP12 Stable Transfection Cell Lines

293/CD33-DAP12 and 293/ΔE2CD33-DAP12 stable transfection cell lines were cultured according to an adapted version of the HEK-293 manufacturer's guidelines. Cells were kept in culture post-transfection or frozen and stored at -80°C to prevent large passage numbers from accruing over time. Frozen cells were thawed quickly in pre-warmed media (Minimum Essential Medium, 10% fetal bovine serum (FBS), 1% sodium pyruvate, 1X non-essential amino acids, 100 I.U./mL penicillin and 100 µg/mL streptomycin, and 400 µg/mL G418). The cells were passaged upon reaching 80-90% confluency by removing media, washing the plate with sterile 1X PBS, and detaching the cells chemically using 0.25% Trypsin/EDTA.

Freezing Cells

Cells were maintained in an actively growing state for at least 48 hours and were free of contamination. Growth media was removed by aspiration and cells were washed using 1X sterile PBS. Cells were lifted off the tissue culture plate chemically using

Trypsin/EDTA by covering cells in a thin layer of trypsin and incubating for 30 seconds at 37˚C. The trypsin was then neutralized after the cells were detached by adding the appropriate serum containing growth medium to the cells, ensuring that the volume added is at least double the volume of the trypsin to ensure neutralization and avoid cell damage. The cell suspension was then collected in a 50mL centrifuge tube and spun in a centrifuge at 1200 rpm for 5 minutes. The media was then aspirated from the tube, leaving the remaining cell pellet. The cell pellet was then resuspended in the appropriate growth media containing 5% dimethyl sulfoxide (DMSO). The resuspended cells were then transferred to a labeled cryogenic vial and placed in a controlled rate cryo-freezing container in a -80°C freezer to ensure the cells freeze down at a rate of approximately 1°C per minute. Once fully frozen, the cell vials were transferred for longer term storage in liquid nitrogen. Cells were then thawed for use as needed.

Cell Treatments

Activation of CD33 was investigated by treating cells with various antibodies or Aβ42 peptide. Adherent cells were seeded into 6-well tissue culture plates for one to two days until 80% confluence. Immediately prior to treatment, media was aspirated, and cells were washed with 1X PBS. Media was replaced with the appropriate serum free media based on the cell line. For suspension cell lines, cells were grown up in a tissue culture flask to 80% confluence. Cells were spun down at 1000 rpm for 5 minutes, washed in 1X PBS, resuspending the cells in the appropriate serum free media. Immediately prior to treatment, the Aβ42 peptide was solubilized in 5% DMSO and ice cold sterile 1X PBS to a working concentration of 100 μM and vortexed for 15s. Cells treated with Aβ42 were treated at a 10 μM concentration for 30 minutes. Antibody

treatments were performed at varying concentrations (5, 10, or 15 µg/mL) and time points (5, 10, 20, or 30 minutes. A list of all antibodies used can be found in Table 3.

Western Blot

Western blot was performed using Cell Signaling Technology, Inc.'s "Western Blotting Protocol". Lysates generated for Western blot were lysed in 1X SDS+DTT (3X sodium dodecyl sulfate, 30X DTT (dithiothreitol), deionized water). 5 µl of each cell lysate was loaded onto a 4-20% SDS-PAGE gel, including 5 µl of a 3:1 mixture combining biotinylated protein ladder (#7727, Cell Signaling Technology, Inc.) to visualize the molecular weights of the tested proteins, with prestained molecular weight marker (59329, Cell Signaling Technology, Inc.) to visually confirmed success of the transfer step. The gels were run on the BioRad V3 system which includes a semi-dry transfer. After transfer, the nitrocellulose membrane was washed briefly with 1X Tris Buffered Saline, 0.1% Tween® 20 (TBS-t) (Cell Signaling Technology, Inc., #9997). The membranes were then incubated in 5% w/v nonfat dry milk (Cell Signaling Technology, Inc., #9999) in 1X TBS-T at room temperature with gentle shaking for one hour. Primaries were diluted in either 5% w/v nonfat dry milk (Cell Signaling Technology, Inc., #9999) or bovine serum albumin (BSA) (Cell Signaling Technology, Inc., #9998), 1X TBS-T based on the manufacturer's recommended protocol. A list of primary antibodies is provided in Table 3. The blots were left to incubate in the diluted primary antibody overnight with gentle shaking at 4°C overnight. All antibodies with catalog numbers were used were diluted to a final concentration of 1:1000. The CD33 E6V7H antibody is not recommended for Western blot by Cell Signaling Technology but was tested between 200-500 µg/mL.

The blots were then washed three times with 1X TBS-T for 5 minutes each. The membranes were then incubated in an HRP-linked rabbit secondary antibody (Cell Signaling Technology, Inc., Anti-rabbit IgG, HRP-linked Antibody #7074 at 1:2000 and HRP-linked anti-biotin (Cell Signaling Technology, Inc., #7075) each at a 1:2000 dilution in 5% w/v nonfat dry milk, TBS-T. The blots were incubated with gently shaking at room temperature for 1 hour. The blots were then washed three times for 5 minutes each with TBS-T prior to imaging. The membranes were then incubated in a 1:1 solution of LumiGLO® and Peroxide (#7003, Cell Signaling Technology, Inc.) for about 1 minute and added onto a transparency film with excess reagent removed. The blots were then developed using a BioRad ChemiDocTM chemiluminescent imager. The images were exposed at 12, 46, and 120 seconds and labeled with Image Lab™ Software (Version 6.1).

Enzyme-Linked Immunosorbent Assay (ELISA)

The ELISAs were performed using Cell Signaling Technology's FastScan™ ELISA protocol. Cell lysates were prepared by lysing cells in 1X Cell Extraction Buffer (69905 FastScan™ ELISA Cell Extraction Buffer (5X), 25243 ELISA Cell Extraction Enhancer Solution (50X), and deionized water). All ELISA kit materials were brought to room temperature and the appropriate buffers were made immediately prior to performing the ELISA. 50ul of each sample cell lysate was added to each well followed by 50ul of the prepared antibody cocktail containing both the capture and detection antibodies for either the FastScan™ Total Syk ELISA Kit (Cell Signaling Technology, Inc. #69824) or FastScan™ Phospho-Syk (Tyr525/526) ELISA Kit (Cell Signaling Technology, Inc. #51426). Sensitivity curves were provided for each product, showing

that the FastScan™ Total Syk ELISA Kit has a 4-fold higher sensitivity than the FastScan™ Phospho-Syk (Tyr525/526) ELISA Kit, so the lysates were diluted by that amount to ensure the total Syk kit could be used as an appropriate loading control. The sample and antibody cocktail were allowed to incubate at room temperature with moderate agitation on a benchtop shaker at 400 rpm. After incubation, the plates contents were discarded and the plates were washed 4 times with 200 µl of 1X ELISA wash buffer (Cell Signaling Technology, Inc., ELISA Wash Buffer (20X) #9801 c diluted to 1X in deionized water). After washing, 100 µl of the TMB Substrate (Cell Signaling Technology, Inc., #7004) was added to each well and allowed to develop in the dark at room temperature with moderate agitation for 15 minutes. Following development, 100 µl of STOP solution (Cell Signaling Technology, Inc., #7002) was added to each well and the plate was lightly shaken prior to reading results. Results were read spectrophotometrically, measuring absorbance at 450 nm.

Table 1: Immortalized cell lines used within this thesis

Cell Line	Tissue	Cell Type	Morphology	Disease
HEK/293	Kidney; Embryo	Epithelial	Epithelial	NA
HMC3	Brain	Microglia	Macrophage	NA
THP-1	Peripheral blood	Monocyte	Monocyte	Acute monocytic leukemia
TF-1	Bone marrow	Erythroblast	Lymphoblast	Erythroleukemia

Table 2: A list of plasmid names and sequences used within this thesis

Plasmid Name	Amino Acid Sequence
CD33-DAP12	MPLLLLLPLLWAGALAMDPNFWLQVQESVTVQEGLCVLVPC TFFHPIPYYDKNSPVHGYWFREGAIISRDSPVATNKLDQEVQE ETQGRFRLLGDPSRNNCSLSIVDARRRDNGSYFFRMERGSTK YSYKSPQLSVHVTDLTHRPKILIPGTLEPGHSKNLTCSVSWAC EQGTPPIFSWLSAAPTSLGPRTTHSSVLIITPRPQDHGTNLTCQ VKFAGAGVTTERTIQLNVTYVPQNPTTGIFPGDGSGKQETRA GVVHMGGLEPCSRLLLLPLLLAVSGLRPVQAQAQSDCSCSTV SPGVLAGIVMGALVLTVLIALAVYFLGRLVPRGRGAAEAATR KQRITETESPYQELQGQRSDVYSDLNTQRPYYK
ΔE2-CD33-DAP12	VHVTDLTHRPKILIPGTLEPGHSKNLTCSVSWACEQGTPPIFS WLSAAPTSLGPRTTHSSVLIITPRPQDHGTNLTCQVKFAGAGV TTERTIQLNVTYVPQNPTTGIFPGDGSGKQETRAGVVHMGGL EPCSRLLLLPLLLAVSGLRPVQAQAQSDCSCSTVSPGVLAGIV MGALVLTVLIALAVYFLGRLVPRGRGAAEAATRKQRITETES PYQELQGQRSDVYSDLNTQRPYYK
WT-CD33 -/+ Myc-DDK	MPLLLLLPLLWAGALAMDPNFWLQVQESVTVQEGLCVLVPC TFFHPIPYYDKNSPVHGYWFREGAIISRDSPVATNKLDQEVQE ETQGRFRLLGDPSRNNCSLSIVDARRRDNGSYFFRMERGSTK YSYKSPQLSVHVTDLTHRPKILIPGTLEPGHSKNLTCSVSWAC EQGTPPIFSWLSAAPTSLGPRTTHSSVLIITPRPQDHGTNLTCQ VKFAGAGVTTERTIQLNVTYVPQNPTTGIFPGDGSGKQETRA GVVHGAIGGAGVTALLALCLCLIFFIVKTHRRKAARTAVGRN DTHPTTGSASPKHQKKSKLHGPTETSSCSGAAPTVEMDEELH YASLNFHGMNPSKDTSTEYSEVRTQ
ΔE2-CD33 -/+ MycDDK	VHVTDLTHRPKILIPGTLEPGHSKNLTCSVSWACEQGTPPIFS WLSAAPTSLGPRTTHSSVLIITPRPQDHGTNLTCQVKFAGAGV TTERTIQLNVTYVPQNPTTGIFPGDGSGKQETRAGVVHGAIGG AGVTALLALCLCLIFFIVKTHRRKAARTAVGRNDTHPTTGSAS PKHQKKSKLHGPTETSSCSGAAPTVEMDEELHYASLNFHGM NPSKDTSTEYSEVRTQ

Table 3: A list of antibodies used within this thesis

Antibody Name	Source & catalog number	Application
CD33 Antibody	Cell Signaling Technology, 77576	Western blot
CD33 (E6V7H) Rabbit mAb (PBS formulation)	Cell Signaling Technology	Cell culture, Western blot
Anti-CD33 Antibody, clone P67.6	Sigma Aldrich Inc., MABF2163	Cell culture
Anti-Human CD33, Purified, (clone: CD33 1C7/1)	Cedarlane Laboratories, CL7627AP	Cell culture
IgM (E9U8J) XP® Rabbit mAb (PBS formulation)	Cell Signaling Technology	Cell culture
Rabbit (DA1E) mAb IgG XP® Isotype Control (PBS formulation)	Cell Signaling Technology	Cell culture
Mouse IgG1, kappa monoclonal [15-6E10A7] Isotype Control (BSA and Azide free)	Abcam, ab221848	Cell culture
SHP-1 (E1U6R) Rabbit mAb	Cell Signaling Technology, 26516	Western blot
Phospho-SHP-1 (Tyr564) (D11G5) Rabbit mAb	Cell Signaling Technology, 8849	Western blot
Phospho-SHP-1 (Tyr564) (D11G5) Rabbit mAb	Cell Signaling Technology, 8850	Western blot
SHP-2 (D50F2) Rabbit mAb	Cell Signaling Technology, 3397	Western blot
Phospho-SHP-2 (Tyr542) (E8D6V) Rabbit mAb	Cell Signaling Technology, 15543	Western blot
Syk (D3Z1E) XP® Rabbit mAb	Cell Signaling Technology, 13198	Western blot
Phospho-Zap-70 (Tyr319)/Syk (Tyr352) (65E4) Rabbit mAb	Cell Signaling Technology, 2717	Western blot
α-Actinin (D6F6) XP® Rabbit mAb	Cell Signaling Technology, 6487	Western blot
β-Actin (D6A8) Rabbit mAb	Cell Signaling Technology, 8457	Western blot
Myc-Tag (71D10) Rabbit mAb	Cell Signaling Technology, 2278	Western blot

Chapter III.

Results

This chapter describes the results of each experiment performed throughout the process of identifying an antibody modulator of the CD33 signaling pathway.

Stable Line Generation

To analyze activation of CD33, two stable cell lines were generated as previously described by Wißfeld et al. One stable line would provide a readout to monitor activation of CD33, and the other stable line was built as a control using a truncated version of the CD33 protein lacking the sialic acid binding domain, thus blocking CD33 activation and mimicking a lack of exon 2.

The plasmid for the positive CD33 readout was designed using the full extracellular CD33 IGV, or sialic acid binding domain, with full-length downstream signaling partner DAP12 attached at the transmembrane region. A modification of DAP12 was made at plasmid design with a mutation of D50A to eliminate any interaction with TREM2 that may impact the CD33 readout. The fusion protein is expected to localize to the membrane, with CD33 located extracellularly and DAP12 intracellularly. This would allow for activation from an external source and downstream signaling to occur endogenously within the cell. The plasmid for the negative CD33 readout was designed using a truncated version of the extracellular portion of CD33, ΔE2-CD33, which lacks the IGV/sialic acid binding domain, with full-length DAP12 attached at the transmembrane region. The sequences for both plasmids are shown in Table 2. The plasmids were designed at Cell Signaling Technology, Inc. and synthesized at Integrated

DNA Technologies, Inc. (IDT). The plasmid concentrations were normalized to 1 µg/µl with the backbone containing the NeoR/KanR gene, allowing mammalian cell selection with Geneticin/G418.

All plasmids were tested by transfecting HEK/293 cells using an optimized version of the Lipofectamine manufacturer's transfection protocol. The transfections were tested by Western blot using antibodies for CD33, DAP12, or β-actin as a loading control (Figure 6). The CD33 antibody, E6V7H, was able to detect both expressed versions of CD33. The E6V7H clone was validated in house at Cell Signaling Technology, Inc. by immunoprecipitation of CD33 from TF-1 cells using E6V7H and analyzing the immunoprecipitation data by Western blot, probing lysates with CD33 Antibody (Figure 5). The DAP12 antibody was able to detect the fusion protein and endogenous DAP12 at 12 kDa (Figure 6, B). A difference in molecular weight between the fusion proteins was seen by Western blot between the CD33-DAP12 and truncated ΔE2-CD33-DAP12, with the ΔE2-CD33-DAP12 fusion protein expressing approximately 10-12 kDa lower than CD33-DAP12.

Once the plasmids were confirmed to be working as expected, the Lipofectamine transfection protocol was optimized before generating the stable cell lines. The CD33-DAP12 and ΔE2-CD33-DAP12 plasmids were transfected into HEK/293 cells at varying concentrations of cDNA (2, 4, or 6 ug) and were kept in transfection for 24 or 48 hr periods before lysing (Figure 7). It was determined that 2 µg of cDNA was the optimal concentration to transfect. The 24-hour transfection appeared to be the most optimal for these transient transfections. However, both 24- and 48-hour transfections were attempted when generating the stable cell lines to account for the difference in protocol.

Prior to generating the stable lines, a kill curve using HEK/293 cells and Geneticin/G418 was established over the course of seven days to choose the most appropriate concentration of selection antibiotic to ensure that, upon selection, cell death will occur in untransfected cells, while cells retaining the desired plasmid continue growth and expansion. The optimal concentration used is the concentration that leads to cell death in all plated cells at day seven, with some cell death visible after just a few days in selection. Based on the dose response curve (Figure 8) it was determined that the initial amount of Geneticin/G418 to be used for selection in HEK/293 cells would be 900 µg/mL.

The stable lines were then generated by transfecting HEK/293 cells and placing the cells under selection 24- or 48-hours post transfection. After the selection process, the cells were expanded into single cell colonies in a 96-well plate. Strong single colony clones were then expanded and grown for additional experiments. Two clones from each of the transfections were confirmed by Western blot to contain CD33 and DAP12 (Figure 9).

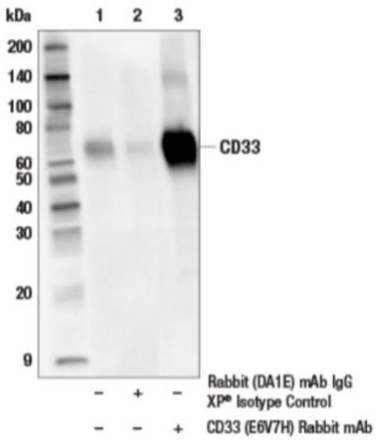

Figure 5: Target specificity validation of CD33 antibody E6V7H antibody

In house data validation of CD33 clone E6V7H from Cell Signaling Technology, Inc. Immunoprecipitation of CD33 protein from TF-1 cell extracts. Lane 1 is 10% input, lane 2 is Rabbit (DA1E) mAb IgG XP® Isotype Control #3900, and lane 3 is CD33 (E6V7H). Western blot analysis was performed using CD33 Antibody.

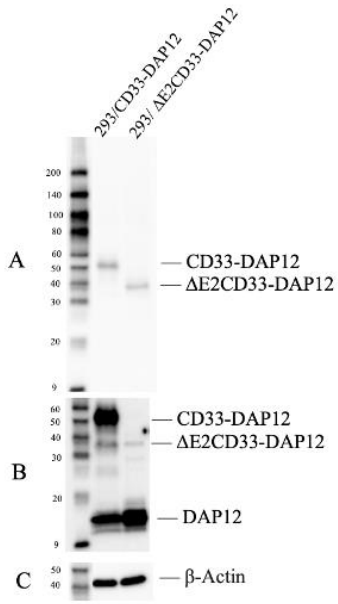

Figure 6: Confirming the CD33-DAP12 and ΔE2-CD33-DAP12 plasmids

Western blot analysis of HEK/293 cells transfected with either CD33-DAP12 or ΔE2-CD33-DAP12 using CD33 E6V7H (A), DAP12 (B), or loading control β-actin (C).

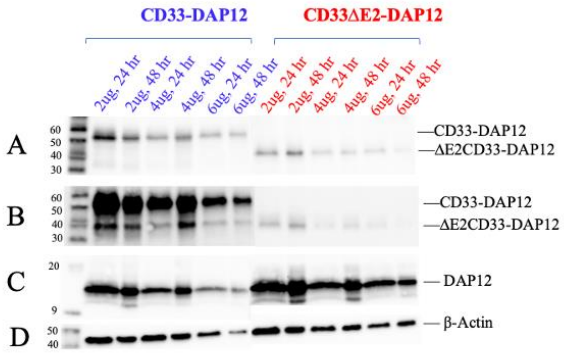

Figure 7: HEK/293 transfection optimization

Western blot analysis of HEK/293 cells transfected for 24 or 48 hours with either CD33-DAP12 or ΔE2-CD33-DAP12 using 2, 4, or 6 μg of DNA using CD33 E6V7H (A), DAP12 (B & C), or loading control β-actin (D). The CD33-DAP12 or ΔE2CD33-DAP12 fusion protein can be seen using CD33 (A) or DAP12 (B). Endogenous DAP12 is also seen in these lysates(C).

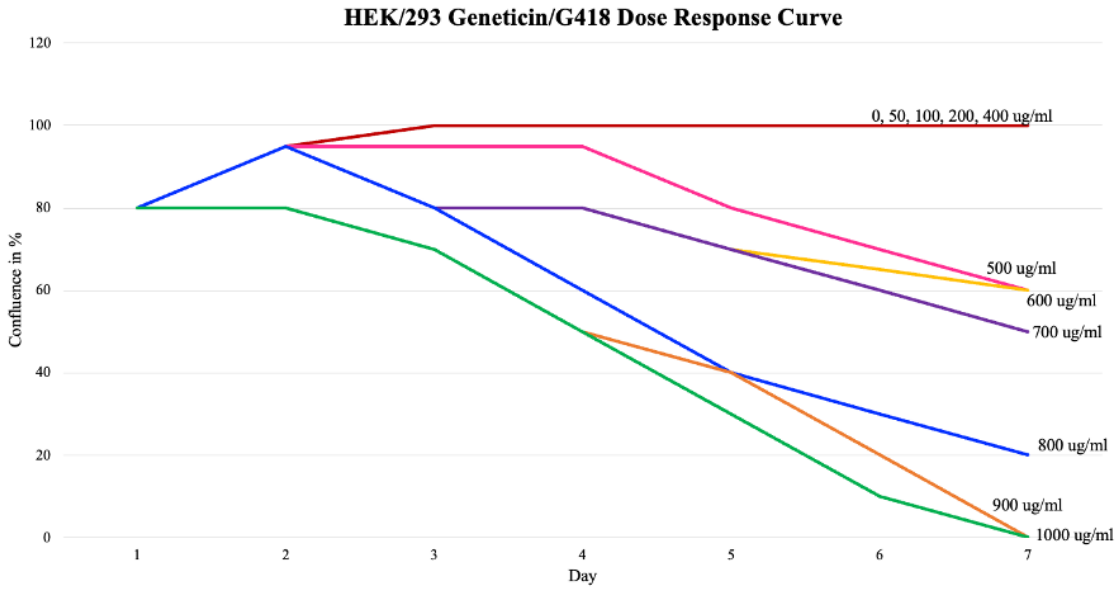

Figure 8: HEK/293 Geneticin/G418 dose response curve

A dose response curve for HEK/293 cells introduced to varying levels of Geneticin/G418 to determine the optimal concentration needed to select for successfully transfected cells to generate a stable cell line. The cells were monitored over the course of 7 days (X-Axis) and measured visually by percent confluence of plated cells (Y-Axis).

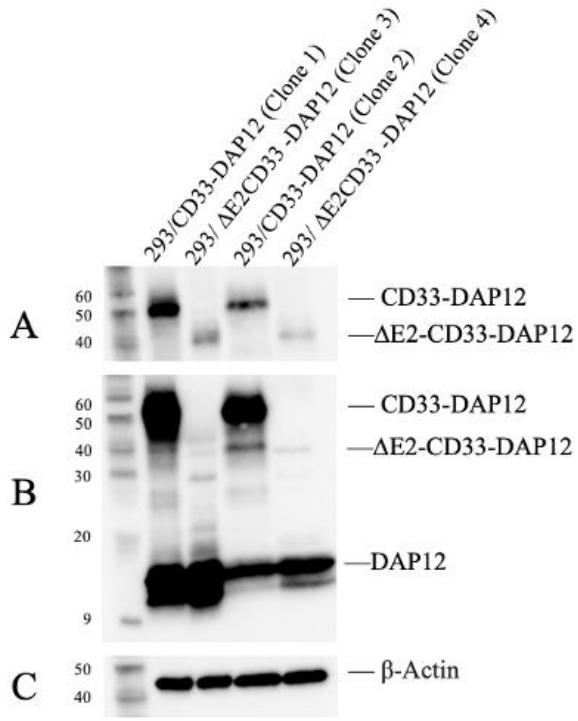

Figure 9: Confirming stable cell lines by Western blot

Western blot analysis of the four generated stable cell lines transfected with either CD33-DAP12 or ΔE2-CD33-DAP12 using CD33 E6V7H (A), DAP12 (B), or loading control β-actin (C).

Optimization of the CD33 Readout

To determine if the stable lines could be used as a readout for CD33 activation as described by Wißfeld et al., the 293/CD33-DAP12 and 293/ΔE2-CD33-DAP12 stable lines and untransfected HEK/293 cells were treated with a previously identified CD33 activating mouse monoclonal antibody, 1c7/1, at varying time points (5, 10, 20, or 30 minutes). The cells were also treated with an IgG1 isotype control antibody to match the 1c7/1 isotype, an IgM rabbit monoclonal antibody to act as a phospho-SYK control, and a previously identified TREM2 rabbit monoclonal antibody shown in-house to activate the TREM2 signaling pathway, or the cells remained untreated. After treatment, the cells were lysed and analyzed by ELISA to test for phosphorylation of SYK at Y525/Y526 (Figure 10). An ELISA for total SYK was also performed to determine total SYK levels in each sample to ensure proper loading. However, the sensitivity of the assay is significantly higher than that of the phospho-SYK ELISA, so too much protein was loaded onto the assay providing an "overflow" result in all lysate loaded wells. While even loading between lanes is unclear based on this result, this confirms that SYK was present in all wells where phospho-SYK (Y525/Y526) levels were negative. This ELISA assay sensitivity was considered for future experiments.

The ELISA readout showed that phospho-SYK (Y525/526) levels were elevated above noise when the 293/CD33-DAP12 cell line was treated with 1c7/1 for 30 minutes. The isotype control nor the TREM2 control produced signal above the untreated 293/CD33-DAP12 sample or the untreated/untransfected 293 cells. There was no significant change above noise in the 293/ΔE2-CD33-DAP12 cell line with any of the treatments. There was no significant difference between cell treatments in the 293/ΔE2-

CD33-DAP12 cell line when compared to the 293 cells alone. The total SYK ELISA showed that equal levels of SYK were present in all samples tested. These results show that the removal of the sialic acid binding domain of CD33 affects CD33's downstream signaling capabilities and shows that we were able to reproduce the Wißfeld et al. results and identify activators of CD33 in this cell model. This assay also determined that the 30-minute antibody treatment was the best time condition for the readout of this model.

Once the optimal time point was established, I looked at the impact of antibody concentration on the phospho-SYK (Y525/526) readout to determine the optimal concentration of antibody needed to activate the CD33 signaling pathway within this model. This round, another previously identified CD33 activating mouse monoclonal antibody was included in the testing, clone P67.6. A rabbit monoclonal antibody for CD33, E67VH, was also added to this experiment. The 293/CD33-DAP12 and 293/ΔE2-CD33-DAP12 stable lines and untransfected 293 cells were treated with each antibody at varying concentrations (5, 10, and 15 µg/mL) for 30 minutes. After treatment, the cells were lysed and analyzed by ELISA to test for phosphorylation of SYK at Y525/Y526 (Figure 11, A & B). The results show that the 293/CD33-DAP12 cells treated with both the P67.1 and the 1c7/1 antibody were able to produce a phospho-SYK (Y525/Y526) reading 1.24 or .3 absorbance units above the untreated control, respectively. The difference in signal between the concentration of antibody is small, however, the absorbance reading does show a positive correlation with the antibody treatment concentration, indicating that the 15 µg/mL concentration in the optimal treatment concentration compared to 5 or 10 µg/mL. Comparing these results to the results produced by Wißfeld, et al., the P67.6 antibody produces a significantly higher phospho-

SYK (Y525/Y526) absorbance when compared to 1c7.1, which replicates previous results. Looking at the phospho-SYK (Y525/526) absorbance reading of the treated 293/ΔE2-CD33-DAP12, results show that there is no difference in signal between the untreated control and any of the antibody treatments. Again, we see no difference between any of the treated 293/ΔE2-CD33-DAP12 samples and the treated 293 control samples. Each sample was also tested on an ELISA for total SYK protein, showing that SYK levels were present and not varying enough to affect the results (Figure 11, C). This strengthens the original hypothesis that removal of the sialic acid binding domain will inhibit CD33 activation and downstream signaling.

An unexpected, but key, result gained from this experiment was the phospho-SYK (Y525/Y526) absorbance reading from 293/CD33-DAP12 cells treated with the CD33 rabbit monoclonal antibody, clone E67VH. This CD33 antibody treatment provided the highest absorbance reading in this experiment, even surpassing the P67.1 treatment sample. The E6V7H treatment did not show any absorbance over noise in either the 293/ΔE2-CD33-DAP12 or the untransfected 293 control cells. While no rabbit IgG isotype control was used in this experiment, the IgM antibody, which did not produce signal over the untreated sample in 293/CD33-DAP12 cells, is also a rabbit monoclonal antibody, providing potential confidence that this antibody may be a robust activator of CD33.

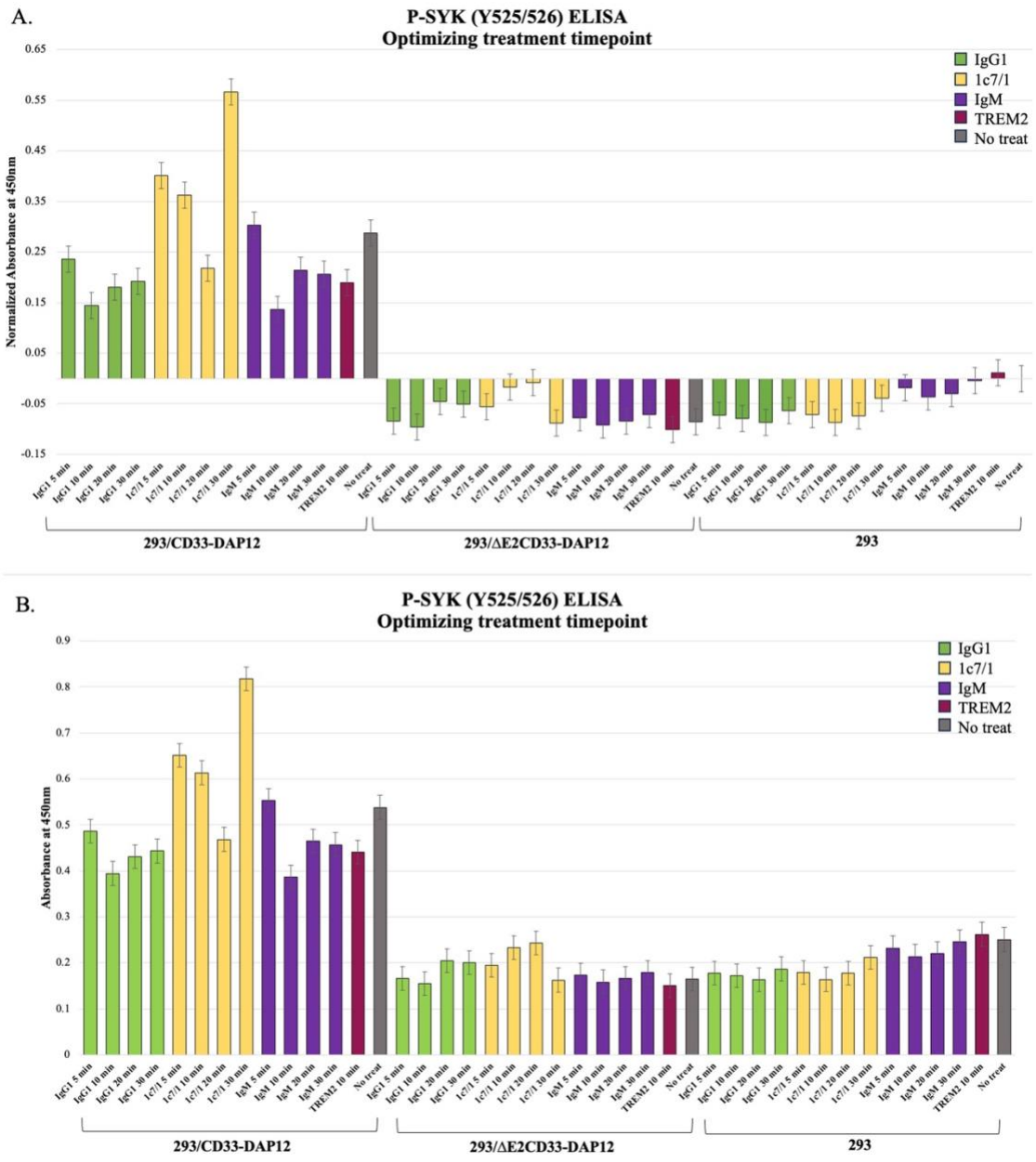

Figure 10: Optimizing treatment timepoint for CD33 activation

A treatment time course of CD33 activation using phospho-SYK (Y525/526) ELISA readout. 293/CD33-DAP12, 293/ΔE2-CD33-DAP12, or 293 cells were untreated or treated with 15 µg/mL IgG1, 1c7/1, IgM, or TREM2 over varying time points (5, 10, 20, or 30 minutes). The samples were measured by absorbance normalized to the untreated 293 sample readout (A) or total absorbance (B).

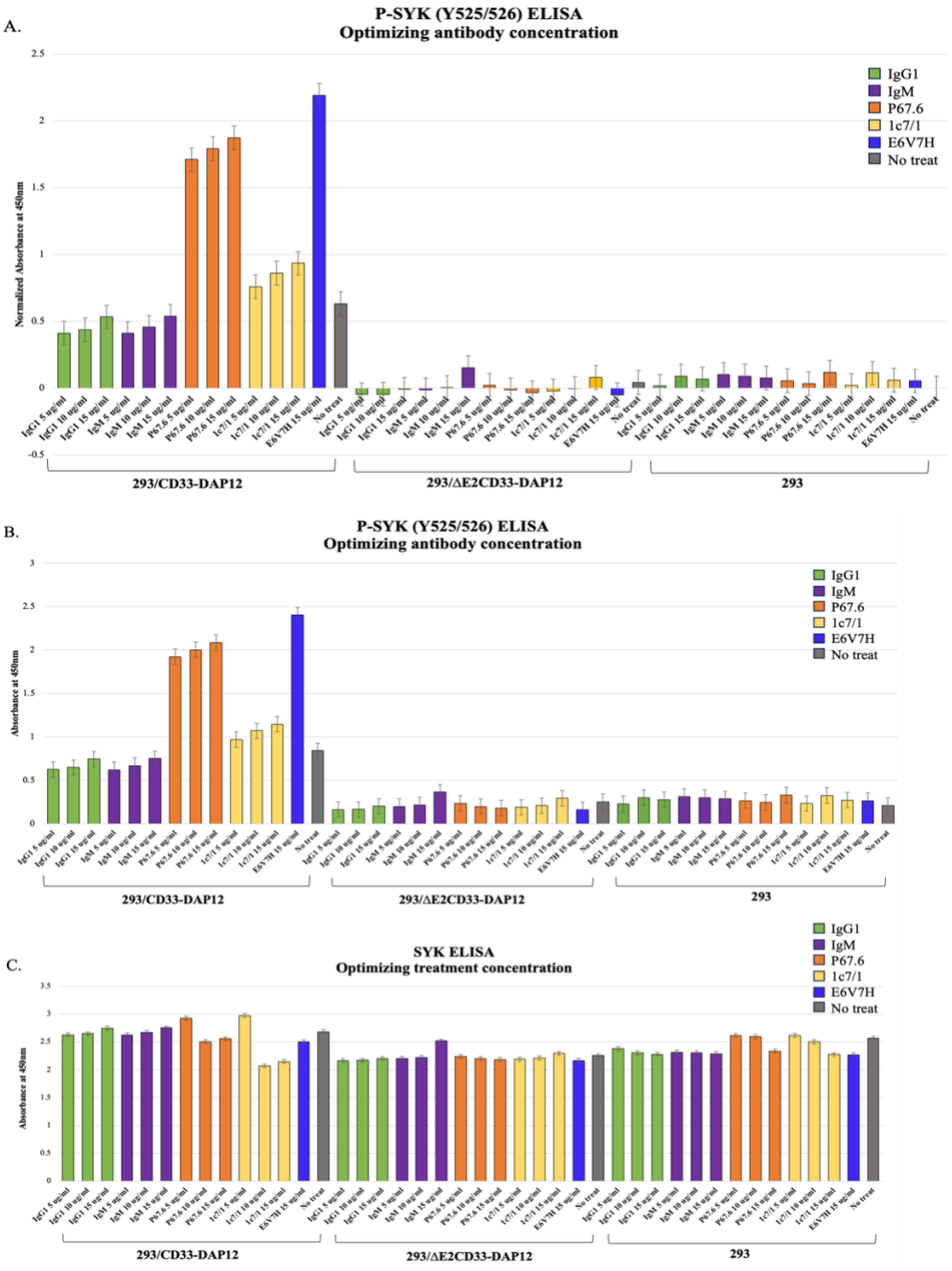

Figure 11: Optimizing treatment antibody concentration for CD33 activation

Treatment optimization of antibody concentration of CD33 activation using phospho-SYK (Y525/526) ELISA readout. 293/CD33-DAP12, 293/ΔE2-CD33-DAP12, or 293 cells were untreated or treated for 30 minutes with IgG1, IgM, P67.6, 1c7/1, or E6V7H at varying concentrations (5, 10, or 15 µg/mL). The samples were measured by absorbance normalized to the untreated 293 sample readout (A) or total absorbance (B). All samples were tested on a total SYK ELISA measuring for absorbance (C).

Testing CD33 Activating Antibodies Using Optimized Protocol

To confirm previously found results, the experiment was repeated using the determined optimal conditions, an antibody concentration of 15 µg/mL for 30 minutes. 293/CD33-DAP12, 293/ΔE2-CD33-DAP12, and untransfected 293 cells were again treated with either an IgG1 isotype control, IgM, P67.6, 1c7/1, or E6V7H. The cell lysates were again analyzed by ELISA, testing for phospho-SYK (Y525/526) (Figure 12). This round of results yielded the same results as the previous experiment, with E6V7H yielding the highest absorbance, P67.6 the second highest, and 1c7/1 yielding results over noise, all a positive readout. Again, no significant signal was seen between any of the treated 293/ΔE2-CD33-DAP12 cells or when compared to the untransfected 293 treatment controls. Repeating this experiment provided more confidence in both the CD33 reporter cell assay model used, and the antibodies' ability to reliably modulate activation of CD33 in this model.

From here, the cell lysates for each treatment and cell line were analyzed by Western blot, looking at total SYK, phospho-SYK (Y525/Y526), phospho-SYK (Y352), with α-actinin acting as a loading control (Figure 13). Total SYK protein was seen in each of the lysates tested across all three cell models (Figure 13, A). Inconclusive signal was seen in the phospho-SYK (Y525/Y526) for the 293/CD33-DAP12 cell line, with completely negative results for both the 293/ΔE2-CD33-DAP12 and 293 cell treatments (Figure 13, B). A band was seen in the phospho-SYK (Y352) panel in the 293/CD33-DAP12 lysates treated with P67.1, 1C7/1, and E6V7H showing a positive result for this SYK phosphorylation site when compared to the untreated and IgG1 control. No signal was seen in the phospho-SYK (Y352) panel for any of the treated 293/ΔE2-CD33-

DAP12 and 293 cell lysates (Figure 13, C). The α-actinin panels showed appropriate even loading across all cell lines tested (Figure 13, D).

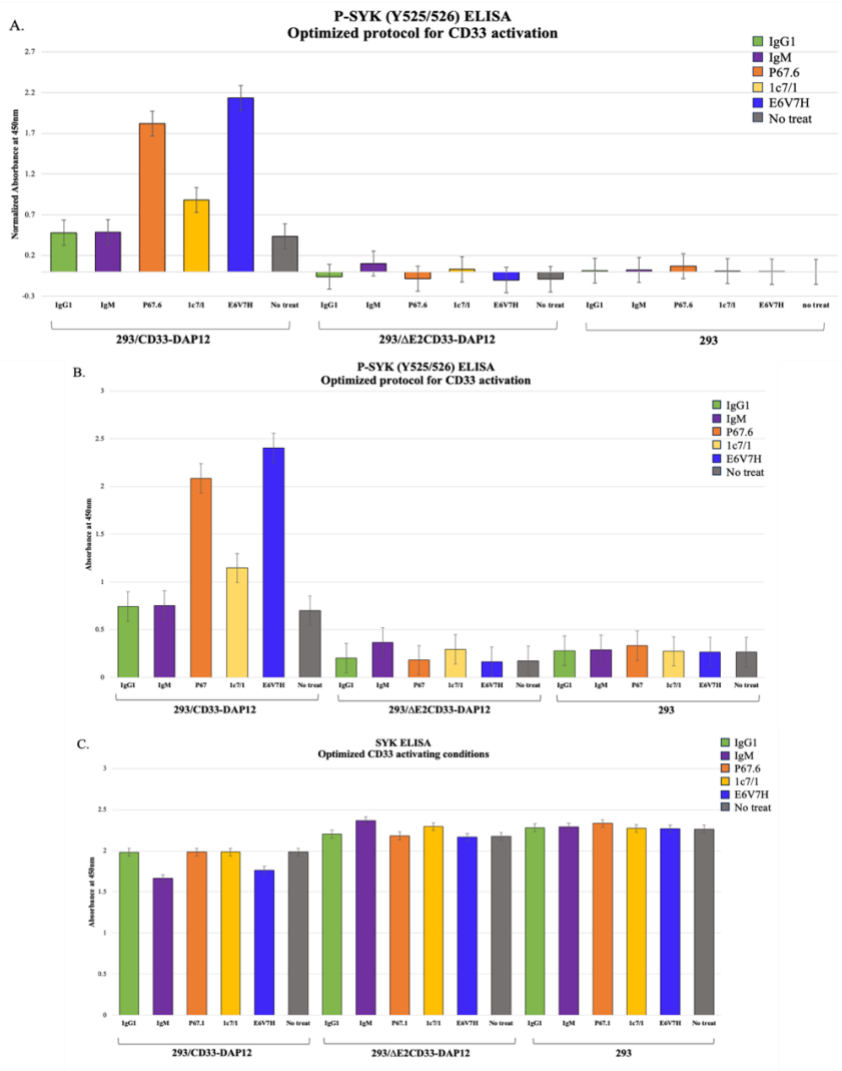

Figure 12: Testing optimized treatment protocol for CD33 activation

Testing previously established optimized treatment protocol of CD33 activation using phospho-SYK (Y525/526) ELISA readout. 293/CD33-DAP12 (blue), 293/ΔE2-CD33-DAP12 (yellow), or 293 cells (green) were untreated or treated for 30 minutes with 15 µg/mL of IgG1, IGM, P67.6, 1c7/1, or E6V7H. The samples were measured by total absorbance (A), or absorbance normalized to the untreated 293 sample readout (B). All samples were tested on a total SYK ELISA measuring for absorbance (C).

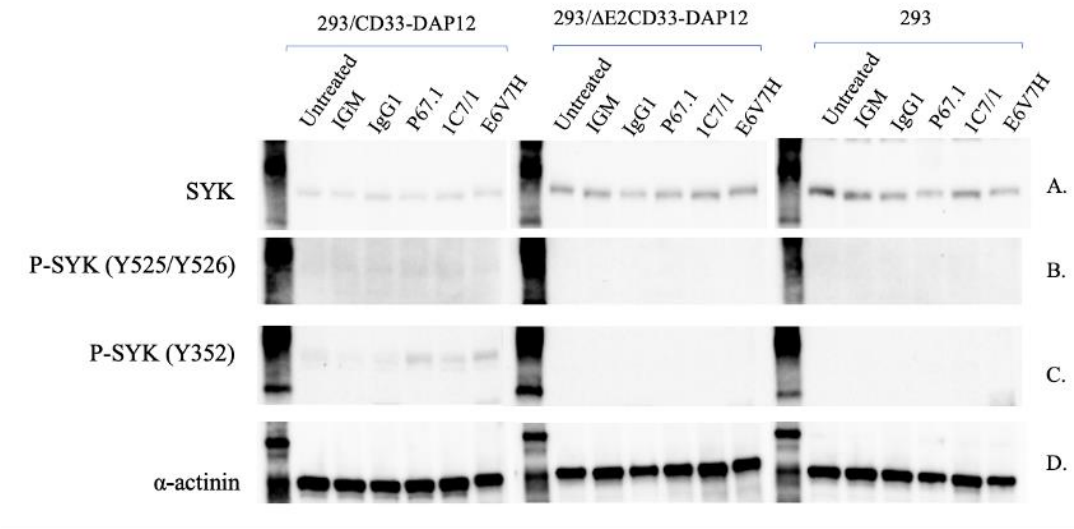

Figure 13: Western blot testing of optimized CD33 activation protocol

Western blot analysis testing the previously established optimized treatment protocol of CD33 activation. 293/CD33-DAP12, 293/ΔE2-CD33-DAP12, or 293 cells were untreated or treated for 30 minutes with 15 µg/mL of IgG1, IGM, P67.6, 1c7/1, or E6V7H. The blots were probed with total SYK (A), phospho-SYK (Y525/526) (B), phospho-SYK (Y352) (C), or α-actinin (D).

Testing Multiple CD33 Antibodies with Varying Epitopes

CD33 antibodies of varying epitopes were tested alongside E6V7H to potentially identify other modulating antibodies for CD33 and explore the epitopes of antibodies that may contain these properties. Two antibodies were chosen within the sialic acid binding V-set domain; one surrounding amino acid P45 and one surrounding S125; and another chosen within the Ig domain surrounding amino acid N160. Another antibody was chosen within the intracellular domain as a control, surrounding amino acid H300. These antibodies are polyclonal and previously confirmed in-house at Cell Signaling Technology to positively identify CD33. An additional control was added for an antibody toward an epitope tag, purified in the same buffer by the same method to act as a control

for the polyclonal antibody samples. Rabbit IgG was utilized as the isotype control. 293/CD33-DAP12, 293/ΔE2-CD33-DAP12, and untransfected 293 cells were all untreated or treated with each of the mentioned CD33 antibodies or antibody controls at a concentration of 15 µg/mL for 30 minutes. The cell lysates were run on an ELISA to detect a readout of phospho-SYK (Y525/Y526) (Figure 14, A & B) or total SYK (Figure 14, C).

None of the newly added CD33 antibodies produced any signal above the untreated control. The E6V7H antibody, however, performed as it had previously with an absorbance relative to the ELISA's included positive control. We hypothesize that the E6V7H antibody epitope may be within the C2-type Ig domain because of its ability to detect both CD33-DAP12 and ΔE2-CD33-DAP12 proteins by Western blot.

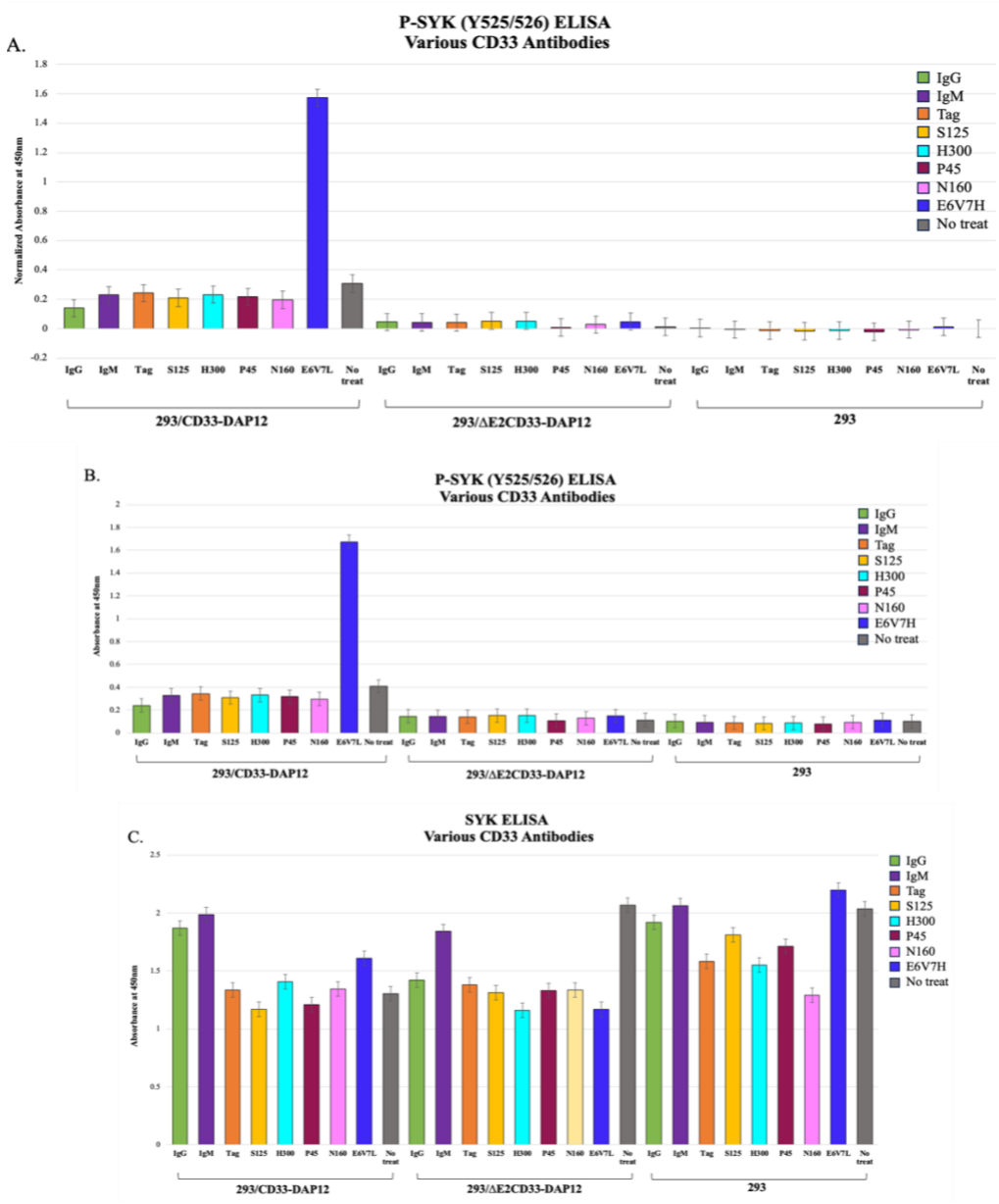

Figure 14: Testing various CD33 antibodies on the optimized protocol

Testing previously established optimized treatment protocol of CD33 activation using phospho-SYK (Y525/526) ELISA readout. 293/CD33-DAP12, 293/ΔE2-CD33-DAP12, or 293 cells were untreated or treated for 30 minutes with 15 µg/mL of rabbit IgG, IGM, an IgG buffer control (Tag), S125, H300, P45, N160 or E6V7H. The samples were measured by absorbance normalized to the untreated 293 sample readout (A) or total absorbance (B). All samples were tested on a total SYK ELISA measuring for absorbance (C).

Comparing Newly Identified CD33 Modulating Antibody, E6V7H, with Aβ42 Peptide

We wanted to compare the newly identified CD33 modulating antibody, E6V7H, with an Alzheimer's disease relevant Aβ42 peptide. It has been shown that Aβ42 binds clustered sialic acid residues on cell surfaces, attenuating AD (Patel et al., 2007). It has also been shown that Aβ42 peptide cell treatments can modulate phagocytosis *in vitro* (Akhter et al., 2020). We treated 293/CD33-DAP12, 293/ΔE2-CD33-DAP12, and untransfected 293 cells with rabbit isotype control IgG, rabbit monoclonal CD33 antibody E6V7H, mouse IgG1 isotype control, mouse monoclonal antibody P67.6, or Aβ42 peptide solubilized in DMSO. All antibody controls were tested at 15 µg/mL concentrations for 30 minutes. The Aβ42 peptide was tested at a concentration of 10uM for 30 minutes. All cell lysates were then run on a phospho-SYK (Y525/Y526) (Figure 15, A & B) or total SYK ELISA (Figure 15, C) measuring absorbance. During this round of testing an additional variable was added to confirm all previously attained results. An additional clone from each of the stable lines (Figure 9) was treated to confirm that the original cell colony clones would behave similarly.

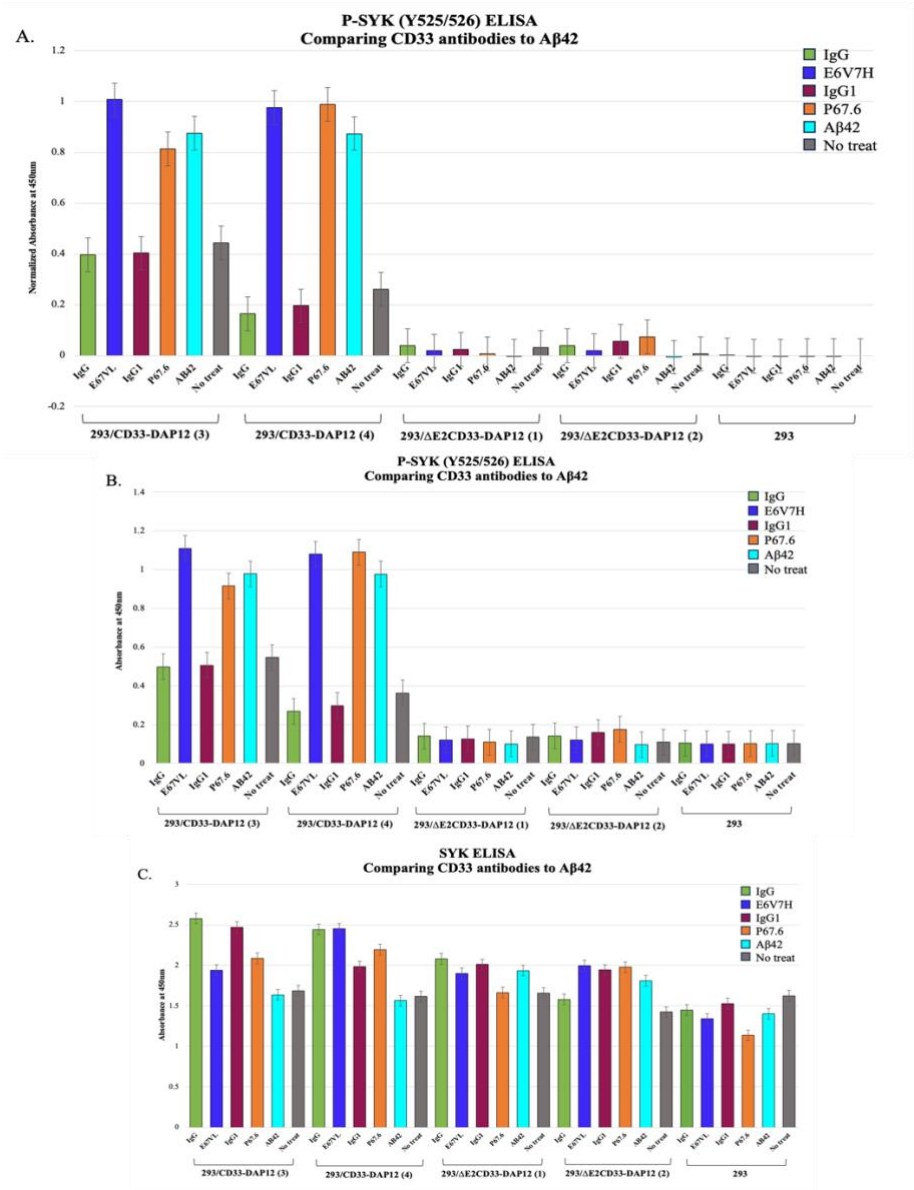

Figure 15: Comparing CD33 activation by CD33 antibodies and Aβ42 peptide

Comparing CD33 activation by CD33 antibodies to Aβ42 peptide and confirming results utilizing additional cell model clones using phospho-SYK (Y525/526) ELISA readout. 293/CD33-DAP12 (3), 293/CD33-DAP12 (4), 293/ΔE2-CD33-DAP12 (1), 293/ΔE2-CD33-DAP12 (2) or 293 cells were untreated or treated for 30 minutes with 15 µg/mL of rabbit IgG, E6V7H, mouse IgG1, P67.6, or 10 Aβ42 peptide. The samples were measured by total absorbance (A), or absorbance normalized to the untreated 293 sample readout (B). All samples were tested on a total SYK ELISA measuring for absorbance (C).

CD33 Activation in Immortalized Human Microglia Cell Line HMC3

To see the effects of CD33 activation in a microglia model, stable transfected cell line generation was attempted with HMC3 cells. The stable lines would contain untagged or MycDDK tagged WT-CD33 or untagged or MycDDK tagged ΔE2-CD33. Studies have shown that HMC3 cells express microglial proteins, including CD33 (Russo et al., 2018). It has also been shown that HMC3 cells can be stimulated to induce phagocytosis of Aβ42 (Butler et al., 2021). However, our results were less substantial using this cell line.

The plasmids were first confirmed by Western blot analysis of HEK/293 transfected cells expressing each of the four plasmids individually (Figure 16). Two CD33 antibodies, CD33 Antibody (Figure 16, A) and E6V7H (Figure 16, B), were confirmed to be present in each transfection. A Myc-tag antibody was used to confirm tag expression in the MycDDK tagged lysates (Figure 16, C). Expected signal was seen in the tagged lysates and no signal was seen in the untagged lysates. β-actin was used as a loading control, confirming even loading across the lysates.

From here, we tested the HMC3 cell line to determine if HMC3 would be a suitable transfection host. Each of the four plasmids was transfected into HMC3 and analyzed by western testing multiple antibodies for (Figure 17). The HMC3 cells were determined to be a suitable transfection host, as they expressed the encoded proteins as expected. CD33 Antibody was used for Western blot analysis because it is capable of more sensitive western detection than E6V7H (Figure 16, A & B). The plasmids transfected into the HMC3 cell line contain the intracellular C-terminal domains of CD33 allowing for use of this antibody with a C-terminal epitope.

To generate the stable cell line, the transfection protocol was then optimized in HMC3 cells. Each lysate was generated using 2ug of cDNA and was lysed 24- or 48-hours post transfection (Figure 18). Based on the results, it was determined that 24 hours post transfection was the optimal protocol.

Prior to attempted the stable cell line, a dose response curve was generated for Geneticin/G418 in HMC3 cells (Figure 19). It was determined that 1000 µg/mL of G418 would be the concentration used for selection.

The stable line protocol was used to attempt generation of HMC3 stable lines expressing WT-CD33 or ΔE2-CD33. Cells were grown to 70% confluency for the transfection. However, the cell morphology is such that the cells group tightly together. Because the cells remained in log phase, when selection was attempted, we hypothesize that the cells were too confluent for the G418 to penetrate the tight cell groups. This stable transfection protocol was attempted again beginning at 50% and 30% confluence. The 50% confluence attempt yielded the same results as beginning at 70%, with tightly grouped colonies. The 30% confluence attempt yielded a very low transfection rate, and cells were not able to fully recover post-selection. The protocol of this process was attempted several more times in a few different ways, such as gentle cell disruption and replating to encourage selection, but none were effective at selecting for transfected HMC3 cells. Based on this, the decision was made to perform cell treatments on transient transfected HMC3 cells instead of an established stable transfected cell line. Since the optimized treatments so far were only 30 minutes long, this was deemed a viable option for the experiment.

Transiently transfected WT-CD33 or ΔE2-CD33 HMC3 cells were treated with either rabbit IgG, IGM, or E6V7L at 15 µg/mL for 30 minutes. These treatments were analyzed by both ELISA testing for phospho-SYK (Y525/Y526) (Figure 20, A) or total SYK (Figure 20, B) and Western blot Western blot (Figure 21). Interestingly, all results were negative. No endogenous levels of SYK were seen in either the Western blot or the total SYK ELISA. The positive and negative controls for the ELISA plate were sound, including additional positive readouts from the endogenous samples described in the next section (Figure 23). On the Western blot, α-actinin was present in the cell lysates generated, confirming that there are HMC3 cells within the treated lysates. Additional HMC3 cell lysates were generated using a separate vial of HMC3 cells. These cell lysates were tested by Western blot using antibodies against SYK, phospho-SYK (Y525/Y526), SHP-1, SHP-2, CD33, DAP12, TREM2, and β-actin (Figure 22). The β-actin control confirms that there is protein in the lysate samples, however, none of the relevant proteins tested were present in the HMC3 cell lysates, other than SHP-2. It remains unclear whether the HMC3 cell line contains the relevant proteins involved in the CD33 pathway based on these results meaning it may not be a suitable cell line to fully test microglia function.

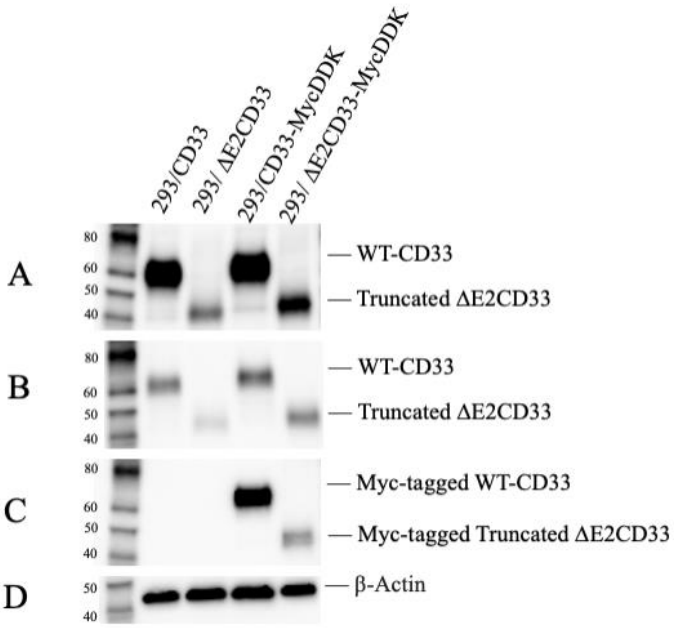

Figure 16: Confirming CD33 plasmids in HEK/293 cells

*Western blot analysis of HEK/293 cells transfected with a plasmid containing CD33, Δ*E2*-CD33, CD33-MycDDK or Δ*E2*-CD33-MycDDK using CD33 Antibody (A), CD33 E6V7H (B), Myc-Tag (C), or loading control β-actin (D).*

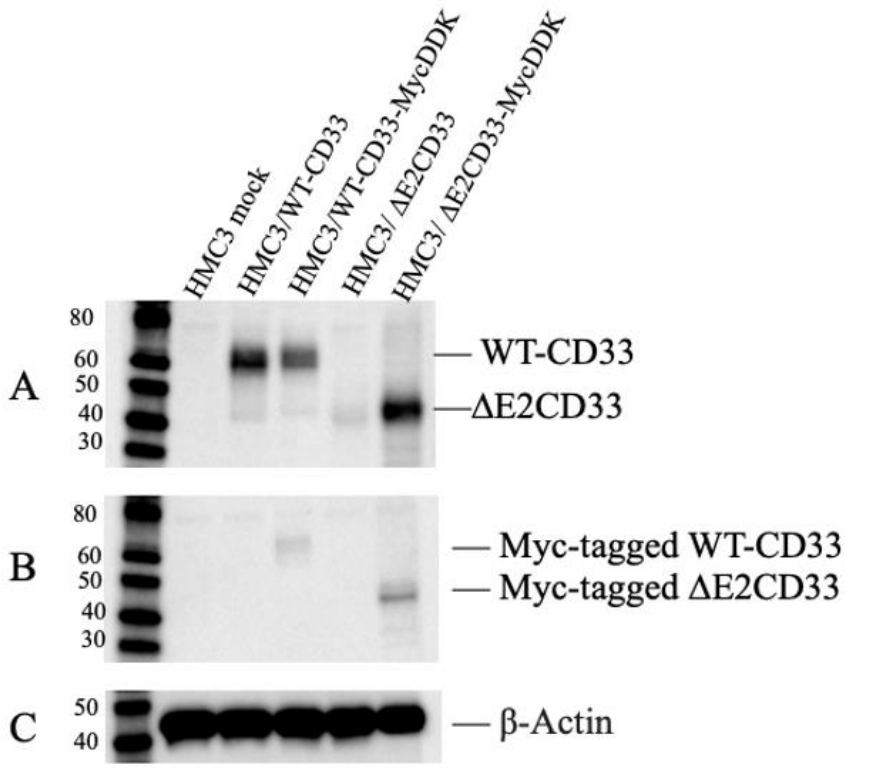

Figure 17: Confirming CD33 plasmids in HMC3 cells

Western blot analysis of HMC3 cells untransfected or transfected with a plasmid containing CD33, ΔE2-CD33, CD33-MycDDK or ΔE2-CD33-MycDDK using CD33 Antibody (A), Myc-Tag (B), or loading control β-actin (C).

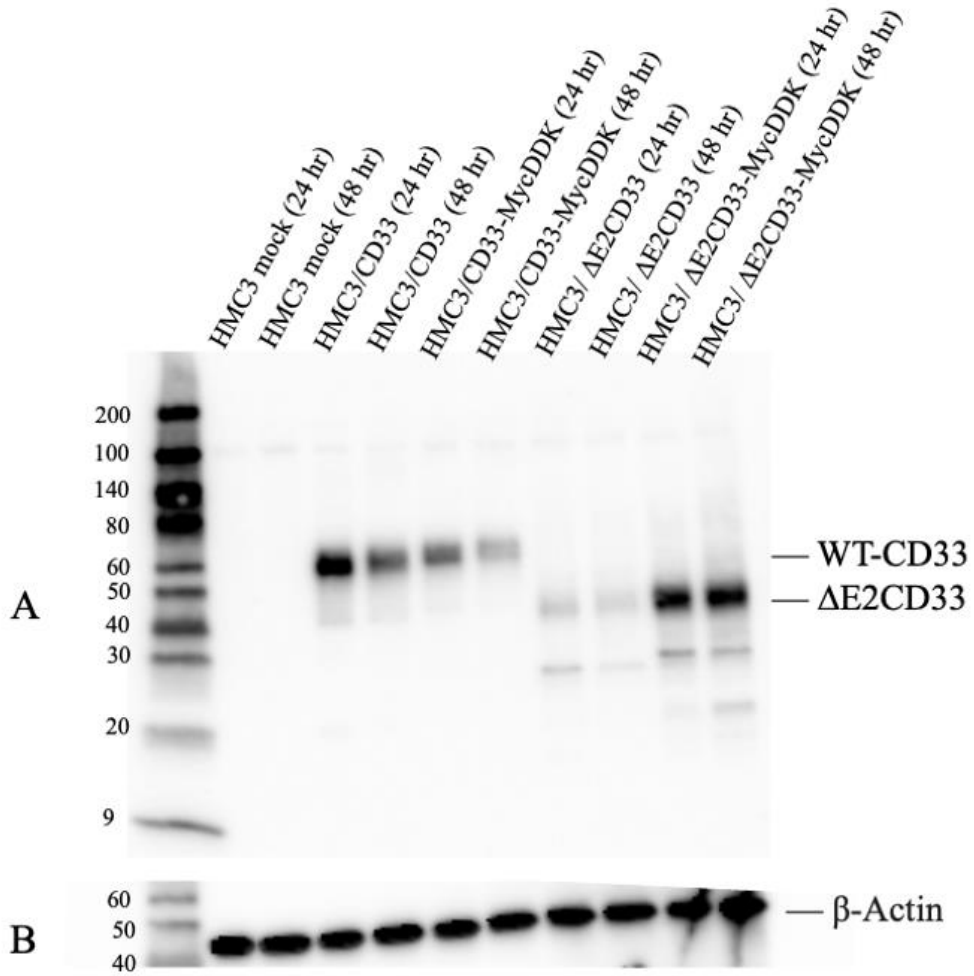

Figure 18: Transfection optimization in HMC3 cells

Western blot analysis of HMC3 cells transfected for 24 or 48 hours with plasmids containing either CD33, ΔE2-CD33, CD33-MycDDK or ΔE2-CD33-MycDDK using 2 μg of DNA using CD33 Antibody (A) or loading control β-actin (B).

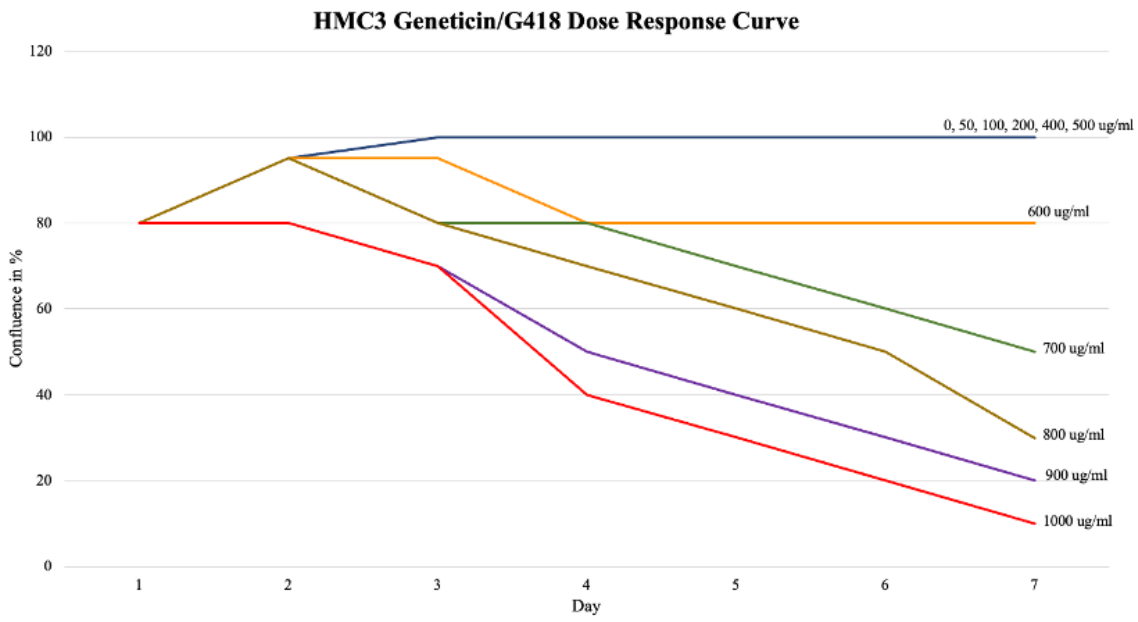

Figure 19: HMC3 Geneticin/G418 dose response curve

A dose response curve for HMC3 cells introduced to varying levels of Geneticin/G418 to determine the optimal concentration needed to select for successfully transfected cells to generate a stable cell line. The cells were monitored over the course of 7 days (X-Axis) and measured visually by percent confluence of plated cells (Y-Axis).

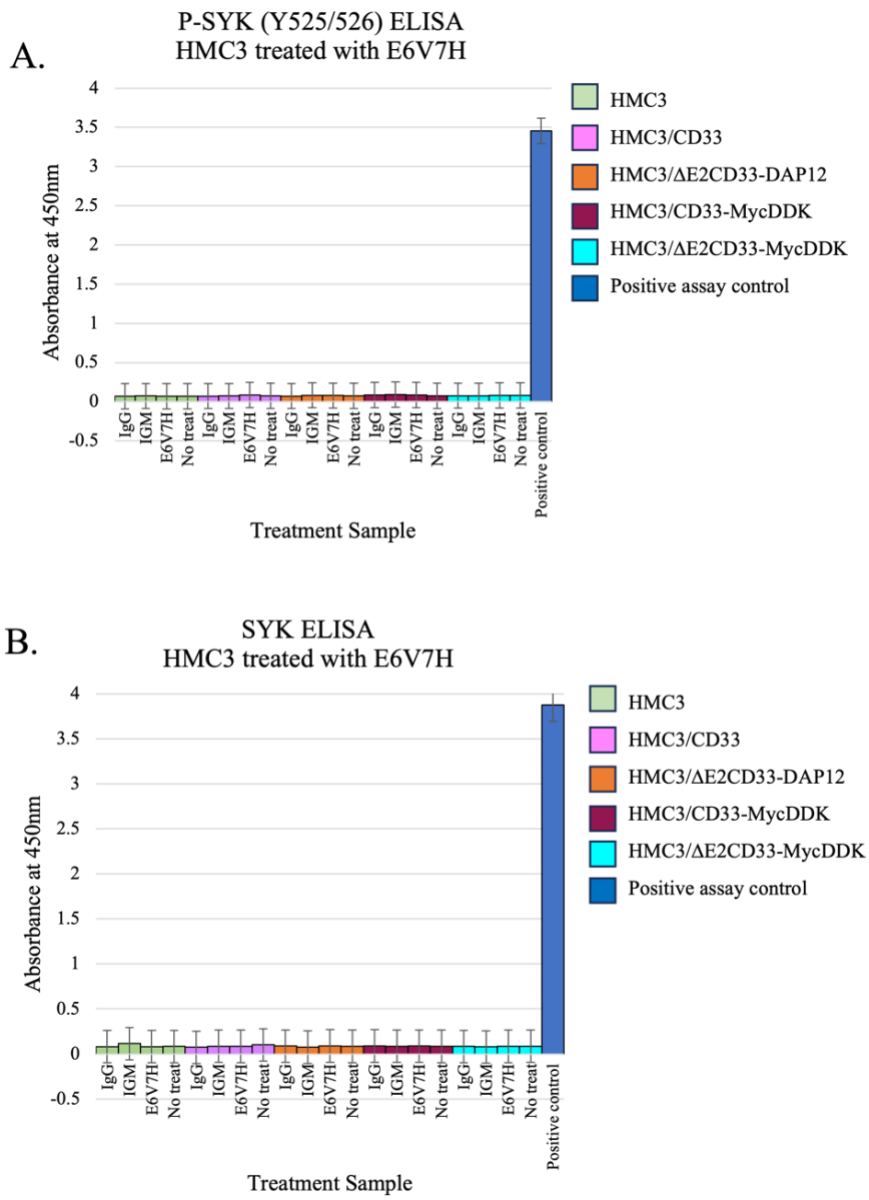

Figure 20: SYK ELISA results for HMC3 treatments

Testing HMC3 cells untransfected or transfected with plasmids containing either CD33, ΔE2-CD33, CD33-MycDDK or ΔE2-CD33-MycDDK. Cells were left untreated or were treated with 15 µg/mL rabbit IgG isotype control or E6V7H for 30 minutes. Cell lysates were tested on a phospho-SYK (Y525/526) or total SYK ELISA. The positive target control provided with the ELISA assay was added to confirm the experiment.

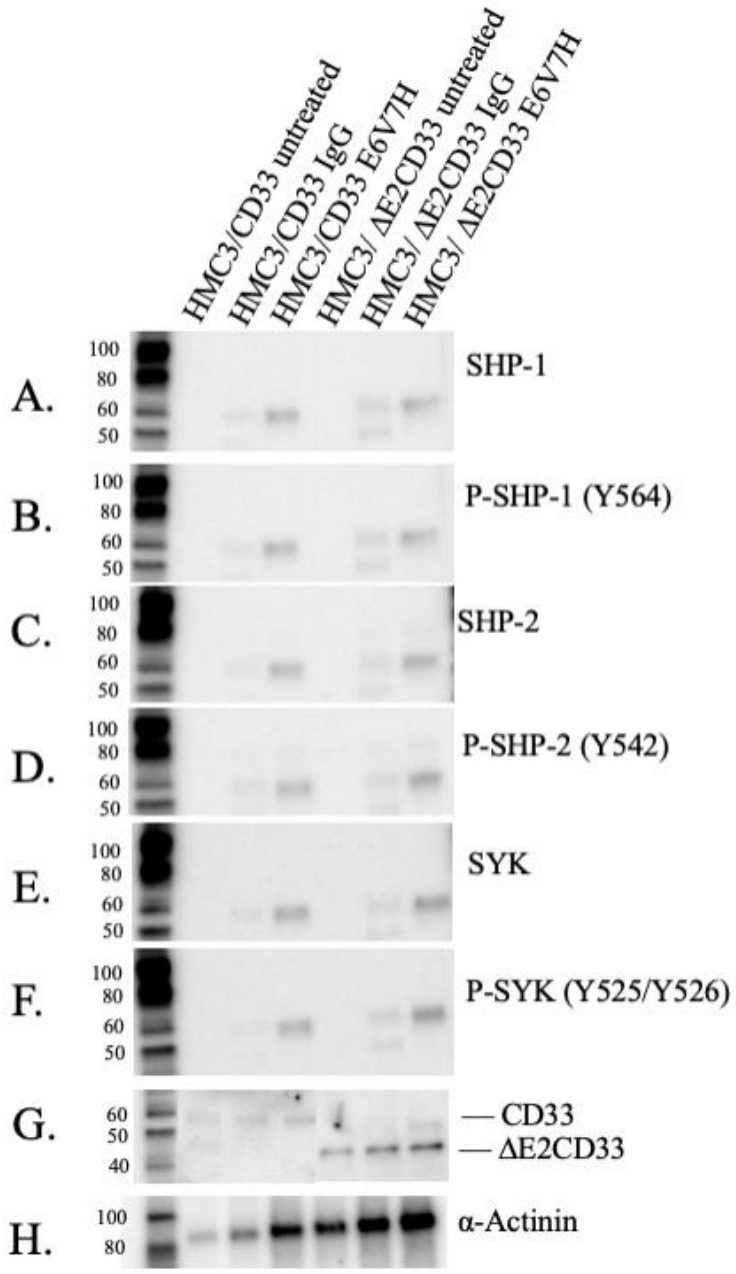

Figure 21: CD33 transfected HMC3 cells treated with E6V7H

Western blot analysis of HMC3 cells transfected with either CD33 or ΔE2-CD33, untreated or treated with rabbit IgG isotype control or E6V7H at 15 µg/mL for 30 minutes, look at SHP-1 (A), phospho-SHIP-(Y564) (B), SHP-2 (C), phospho-SHP-2 (D), SYK (E), phospho-SYK (Y525/Y526) (F), CD33 antibody (G), or loading control α-actinin (H).

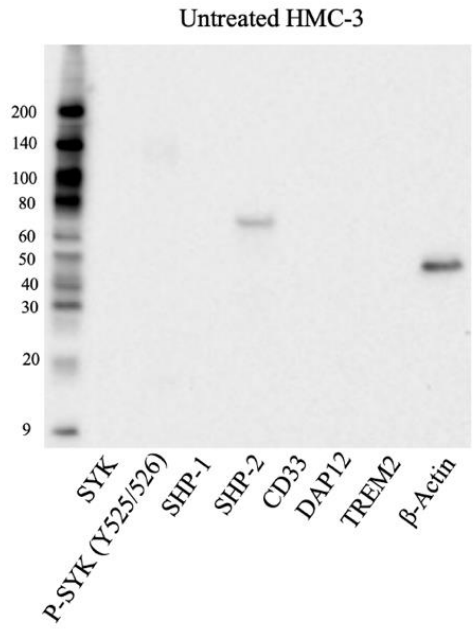

Figure 22: Confirming CD33 pathway protein expression in HMC-3 cell lysate

Western blot analysis of HMC-3 cell lysates probed with primary antibodies SYK, phospho-SYK (Y525/526), SHP-1, SHP-2, CD33, DAP12, TREM2, or β-Actin.

CD33 Activation in Endogenous *In Vitro* Models

To explore potential endogenous CD33, CD33 expressing THP-1 and TF-1 cells were treated with previously established activating CD33 antibody, E6V7H. If successful, it was expected that SHP-1 and/or SHP-2 levels would increase, and phospho-SYK (Y525/526) levels would decrease or remain negative. The cell treatments were tested by ELISA, where significant levels of total SYK were seen (Figure 23, B), while no phospho-SYK (Y525/526) was seen in any treated or untreated sample (Figure 23, A). This result shows that there is SYK present in the samples with no phospho-SYK as

predicted. However, the antibody treatment effect remains inconclusive due to the lack of positive control in these models.

Another optimization of CD33 activation was performed on the endogenous model. Keeping the concentration at 15 µg/mL, a time course was performed with the antibody concentration at 15 µg/mL. Cell lysates were analyzed by Western blot and tested with SHP-1, phosho-SHP-1 (Y564), and α-actinin as the loading control (Figure 24). The results show that total SHP-1 levels increase upon treatment with the E6V7H antibody, with even loading confirmed by α-actinin. The Western blot also shows that the phospho-SHP-1 (Y564) initially decreases compared to the untreated controls, and then signal increases over time (Figure 24, B). The untreated TF-1 showed significant levels of phospho-SHP-1 (Y564), which we hypothesized may have been due to the timing of the cells left in serum free media.

This experiment was repeated, this time removing the 20-minute time point but adding an additional untreated control; untreated serum starved for 5 minutes, or untreated serum starved for 30 minutes to determine if the timing in serum free media had any effect on SHP-1 phosphorylation (Figure 25). Interestingly, we saw the same result. An increase in total SHP-1 was seen upon treatment with E6V7H and a drop with a steady increase was seen again in the phospho-SHP-1 (Y564) blot, especially in the TF-1 cells. This round of western testing, SHP-2 and phospho-SHP-2 (Y542) were added to the experiment. Total SHP-2 levels appear to remain stable in untreated compared to treated lysates. However, the SHP-2 (Y542) appears to increase with the treatment of E6V7H. A slight difference in total SHP-1 was seen between the two untreated controls.

However, the 30-minute treatment loading control is slightly lower than the 5-minute treatment, which may have been the reason behind that.

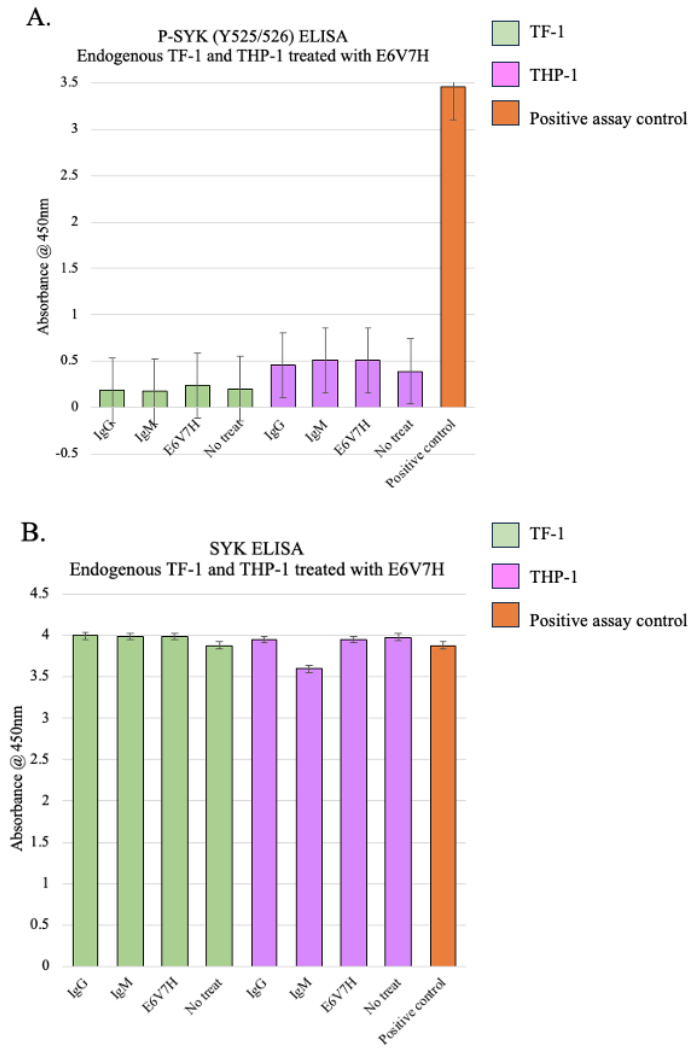

Figure 23: Testing SYK and phospho-SYK levels of treated endogenous CD33 models

Testing phospho-SYK (Y525/526) (A) or total SYK (B) levels of TF-1 or THP-1 cells untreated or were treated with 15 µg/mL rabbit IgG isotype control or E6V7H for 30 minutes. Cell lysates were tested on a phospho-SYK (Y525/526) or total SYK ELISA. The positive target control provided with the ELISA assay was added to confirm the experiment.

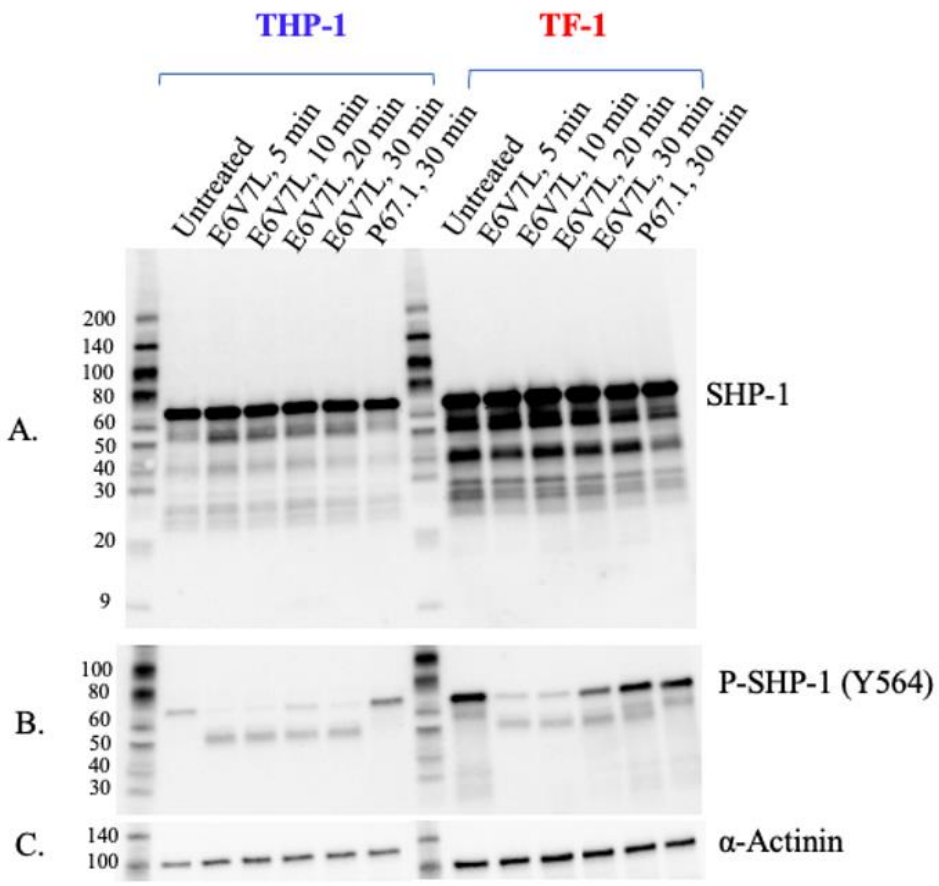

Figure 24: Optimizing CD33 activation in endogenous models using E6V7H

Western blot analysis of THP-1 (left) or TF-1 (right) untreated or treated with 15 µg/mL E6V7H at varying timepoints (5, 10, 20, or 30 minutes), or P67.1 for 30 minutes looking at SHP-1 (A), phospho-SHP-1 (Y564) (B), or α-actinin (C).

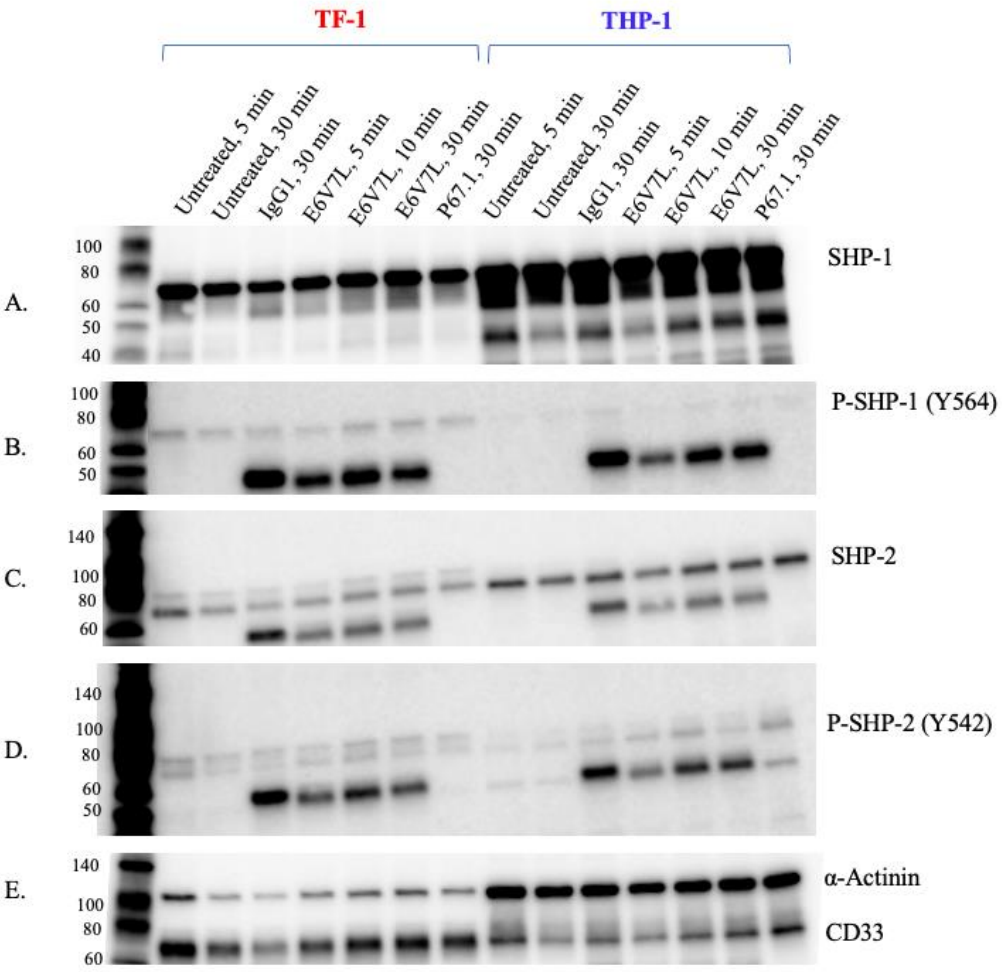

Figure 25: Repeated treatment optimizing for CD33 activation in endogenous models

Western blot analysis of TF-1 (left) or THP-1 (right) untreated or treated with 15 µg/mL E6V7H at varying timepoints (5, 10, or 30 minutes), or P67.1 for 30 minutes looking at SHP-1 (A), phospho-SHP-1 (Y564) (B), SHP-2 (C), phospho-SHP-2 (Y542) (D), CD33 or α-actinin (E).

Chapter IV.

Discussion

The goal of this project was to identify a robust antibody modulator of CD33 in *in vitro* models to enable further investigation into the CD33 signaling pathway and its impact in neurodegenerative disease. CD33 has been implicated in Alzheimer's disease in multiple ways. CD33 expression is positively correlated to beta-amyloid plaque burden. Single nucleotide polymorphisms (SNPs) of CD33 have been identified in genome wide association studies of AD, with SNPs that are implicated in disease and others that are protective against disease (Naj et al., 2011). These SNPs are ultimately linked to a truncated version of CD33, lacking extracellular the sialic acid binding domain. Studies have shown that this truncation may be a gain of function, utilizing the same signaling pathway as downstream protein, TREM2, to encourage phagocytosis of Aβ peptides (Bhattacherjee et al., 2021).

To monitor CD33 activation and identify antibody modulators, a reporter cell assay was developed based on a previous established model by Wißfeld et al. (2021), utilizing a fusion protein of the CD33 extracellular domain linked from its transmembrane region to downstream signaling partner, DAP12. Additionally, the truncated CD33 isoform (D2-CD33 or ΔE2-CD33) lacking the sialic acid binding domain was also generated and linked to DAP12. These fusion proteins were stably transfected into HEK/293 cells to act as the reporter cell assays to monitor CD33 activation through a downstream readout of phospho-SYK (Y525/526).

We were able to confirm the use of the reporter cell assay by replicating the experiments performed by Wißfeld et al. (2021) by using two antibody modulators, 1c7/1 and P67.6, showing that the model was sound. The level of activation seen in the phospho-SYK readout was higher in P67.7 when compared to 1c7/1 which replicated their results (Wißfeld et al., 2021).

In addition to confirming previously established modulators of CD33, we were able to identify another robust CD33 activator that worked well in this model. E6V7H is a rabbit monoclonal antibody used within the study that was able to generate phospho-SYK readings similar or higher than P67.6. We were also able to compare these antibodies to modulation by Aβ42 peptides, which performed similarly in the phospho-SYK readouts. While the Aβ42 peptide confirmation was not confirmed, based on the protocol used the structure was likely unaggregated Aβ42 (Stine et al., 2011).

Wißfeld, et al. also determined the epitopes of the antibodies and mapped 1c7/1 to the C2-IgG domain, and P67.6 to the sialic acid binding domain. This was determined based on the antibodies abilities to detect the fusion proteins. The P67.6 antibody could only detect the full extracellular domain of CD33 with the sialic acid binding domain intact, while 1c7/1 was able to detect both fusion proteins. Because the fusion proteins lack the intracellular region of the CD33 protein, the epitope for 1c7/1 can be mapped to the C2-type domain. Interestingly, E6V7H is also able to detect both extracellular CD33 fusion proteins, meaning its epitope is highly likely to be within the C2-type domain. Due to the therapeutic interest in CD33 both in the neuroscience and cancer space, the C2-type domain is highly sought after in antibodies to capture multiple isoforms of CD33 (Godwin et al., 2021). Although the two antibody epitopes can be mapped to the same

domain, they do show a difference in ability to activate downstream signaling. Interestingly, the E6V7H antibody was shown to perform similarly or better than the sialic acid binding domain recognizing P67.6 clone. It was originally hypothesized that antibodies recognizing the sialic acid binding domain would outperform those that recognize the C2-IgG domain. The mechanism by which these antibodies activate CD33 remains unknown and further information is needed to understand why there are differences in CD33 modulation ability between similar and differing domain epitopes.

One area of this thesis that was not investigated, was confirming that the stable cell lines expressed the CD33-DAP12 fusion protein in the cell membrane, allowing for extracellular activation and intracellular signaling providing the phospho-SYK downstream readout. This could have been accomplished by visualizing the cells by immunofluorescence and staining with a compatible CD33 and DAP12 antibody or by flow cytometry on either fixed or live cells. This would aid in confirming the results we saw within this thesis and is worth confirming with future experiments.

The HMC3 experimental results were not as originally expected. The HMC3 cell line proved to be an acceptable transfection host, but I was not able to generate a stable cell line using HMC3. The protocol was modified several times to attempt to create a stable line using HMC3. However, an appropriate protocol was not established within this thesis. A dose response curve for Geneticin/G418 was established for HMC3, with cell death occurring over time beginning at 80% confluence. The issue with generating the stable line seemed to be with establishing the right cell confluence to allow for the cells to effectively transfect in log phase while also allowing for the selection antibiotic to penetrate the cell clusters and remove untransfected cells. Too little cell confluence at

transfection caused the cells to die very quickly during the transfection, but a confluence that was too high lead to the cells clustering and seemingly not being penetrated by the antibiotic. Attempts to gently disrupt the cells were made to introduce the antibiotic, but the cells were not able to adhere back to the plate following the disruption and the cell line could not be established. This is why transient transfection protocols were used for this cell line.

Unexpectedly, after testing the HMC3 cell line, it was found that the cells contained no SYK, SHP-1, CD33, DAP12, or TREM2 protein, making a readout of CD33 activation impossible. It is unclear at this time if the HMC3 cell line itself does not contain these proteins, or if there is an issue with the specific cells obtained for this experiment. Previous studies have used this model for microglial based experiments, including functional assays (Russo et al., 2018; Butler et al., 2021). The cells were maintained in the recommended media and were free of contamination. Visually, the cells matched the expected morphology of the HMC3 cell line. If this model was to be used in the future, a new vial of cells would be ordered, potentially from a different source and thoroughly tested for microglia proteins to determine if the results obtained were specific to our cell stock or the cell line in general.

CD33 activation was also attempted in endogenous models, THP-1 and TF-1. The readout for endogenous activation of CD33 proved to be challenging to decipher. We looked at levels of SHP-1 activation through phosphorylation of SHP-1 at Y564, and compared it to total SHP-1 protein levels by Western blot. This Y564 site has been shown to be critical for SHP-1 phosphatase activity in myeloid cells (Abram & Lowell, 2017). The signal appears to be strong in untreated cells, decrease upon the initial E6V7H 5-

minute treatment, and then appears to increase again correlating with the length of the treatment. The strong decrease in signal was unexpected, as we expected to only see an increase in Y564 representing an increase in SHP-1 activation. However, when the experiment was repeated we saw the same pattern again. While it remains unclear why this result is seen, it is possible that this reflects what is occurring in the CD33 signaling pathway, especially because the result was reproducible. There may be more going on within the recruitment of SHP-1 that requires further exploration.

Another interesting result seen was, upon treatment with E6V7H, an increase in endogenous SHP-1 levels was seen, which was reproducible when a second set of treatments was performed. This increase in protein level requires further investigation because it does not seem plausible that the antibody treatment would increase protein levels in just a matter of minutes. This result may be a coincidental, however, further investigation is required to fully understand why this result occurred and if there is any relationship between the increase in total SHP-1 levels and the decrease in phospho-SHP-1 (Y564).

A strong readout for a specific biomarker indicating endogenous CD33 activation would be helpful for this type of study. Performing proteomic analysis on cells treated by these activating antibodies would provide interesting information into the proteomic changes between treated and untreated cells. Additionally, exploring specific phosphorylation sites indicative of CD33 activation and generating modification specific antibodies toward those sites would be beneficial in continuing this study. Further investigation of other downstream pathways like the PI3 Kinase/Akt pathway (Figure 3) could provide another means of monitoring CD33 activity. Cytokine secretion could also

be measured to monitor macrophage activity in endogenous CD33 models. Previous studies have utilized phagocytosis assays to understand the implication of CD33 truncation on phagocytosis (Bhattacherjee et al., 2021). This type of assay utilizing a fluorescent Aβ peptide could be an interesting functional assay to monitor CD33 activation and its impact on phagocytosis. Overall, additional means of monitoring CD33 activation will be helpful in further validating the identified activating CD33 antibodies to enable further investigation into CD33's impact in disease.

Further, generating a knockout cell model of CD33 in endogenously expressing cell lines like THP-1 or TF-1 would be helpful to confirm the results of this study. This option was explored; however Clustered Regularly Interspaced Short Palindromic Repeats (CRISPR) knockout of suspension cell lines is still a challenge. Wardyn, et al. (2021) has established a protocol for CRISPR-Cas9 gene editing in suspension cell lines, which could be explored as a method in future experiments. It would also be interesting to explore the ability to manipulate CD33 in endogenous cell models, introducing modifications replicating the SNPs found in AD to further explore the signaling mechanism behind the potential gain of function with the E2-CD33 isoform. This would be hugely beneficial to the field to explore the possibilities of CD33 therapeutics and would also aid in confirming CD33 modulators like the antibodies described in this study.

Overall, this thesis strongly suggests that E6V7H, a rabbit monoclonal antibody generated against the amino terminus of CD33, is capable of activating CD33 through its N-terminal domains. This thesis shows that E6V7H is capable of activating CD33 in a reporter cell assay of CD33 activation by increasing the downstream readout within the model in a way that replicates previous findings. Endogenous results suggest that the

proteins involved in downstream CD33 signaling are increased upon stimulation with E6V7H. However, more work on the endogenous models can be done to confirm this antibody's ability to modulate human CD33.

References

Abram, C. L., & Lowell, C. A. (2017). Shp1 function in myeloid cells. *Journal of Leukocyte Biology*, *102*(3), 657–675.

Akhter, R., Shao, Y., Formica, S., Khrestian, M., & Bekris, L. M. (2021). TREM2 alters the phagocytic, apoptotic and inflammatory response to Aβ42 in HMC3 cells. *Molecular Immunology*, 131, 171–179.

Bhattacherjee, A., Jung, J., Zia, S., Ho, M., Eskandari-Sedighi, G., St. Laurent, C. D., McCord, K. A., Bains, A., Sidhu, G., Sarkar, S., Plemel, J. R., & Macauley, M. S. (2021). The CD33 short isoform is a gain-of-function variant that enhances Aβ1–42 phagocytosis in microglia. *Molecular Neurodegeneration*, 16(1), 1–19.

Breijyeh, Z., & Karaman, R. (2020). Comprehensive Review on Alzheimer's Disease: Causes and Treatment. *Molecules*. 25(24), 5789.

Butler, C. A., Thornton, P., & Brown, G. C. (2021). CD33M inhibits microglial phagocytosis, migration and proliferation, but the Alzheimer's disease-protective variant CD33m stimulates phagocytosis and proliferation, and inhibits adhesion. *Journal of Neurochemistry*, 158(2), 297–310.

Crocker, P. R., Paulson, J. C., Varki, A. (2007). Siglecs and their roles in the immune system. *Nature Reviews Immunology*, 7(4), 255–266.

Cummings, J. (2023). Anti-Amyloid Monoclonal Antibodies are Transformative Treatments that Redefine Alzheimer's Disease Therapeutics. *Drugs*, 83(7), 569–576.

Cummings, J.L., Morstorf, T., & Zhong, K. (2014). Alzheimer's disease drug-development pipeline: few candidates, frequent failures. *Alzheimer's Research & Therapy*, 6(4), 37–37.

Estus, S., Shaw, B. C., Devanney, N., Katsumata, Y., Press, E. E., & Fardo, D. W. (2019). Evaluation of CD33 as a genetic risk factor for Alzheimer's disease. *Acta Neuropathologica*, 138(2), 187–199.

Efthymiou, A. G., & Goate, A. M. (2017). Late onset Alzheimer's disease genetics implicates microglial pathways in disease risk. *Molecular Neurodegeneration*, *12*(1), 43–43.

Gao, H-M., & Hong, J.-S. (2008). Why neurodegenerative diseases are progressive: uncontrolled inflammation drives disease progression. *Trends in Immunology*, 29(8), 357–365.

Gauthier, S., Albert, M., Fox, N., Goedert, M., Kivipelto, M., Mestre-Ferrandiz, J., & Middleton, L. T. (2016). Why has therapy development for dementia failed in the last two decades? *Alzheimer's & Dementia*, 12(1), 60–64.

Godwin, C. D., Laszlo, G. S., Fiorenza, S., Garling, E. E., Phi, T.-D., Bates, O. M., Correnti, C. E., Hoffstrom, B. G., Lunn, M. C., Humbert, O., Kiem, H.-P., Turtle, C. J., & Walter, R. B. (2021). Targeting the membrane-proximal C2-set domain of CD33 for improved CD33-directed immunotherapy. *Leukemia*, 35(9), 2496–2507.

Griciuc, A., Patel, S., Federico, A. N., Choi, S. H., Innes, B. J., Oram, M. K., Cereghetti, G., McGinty, D., Anselmo, A., Sadreyev, R. I., Hickman, S. E., El Khoury, J., Colonna, M., & Tanzi, R. E. (2019). Trem2 acts downstream of CD33 in modulating microglial pathology in Alzheimer's disease. *Neuron*, 103(5).

Griciuc, A., Serrano-Pozo, A., Parrado, A. R., Lesinski, A. N., Asselin, C. N., Mullin, K., Hooli, B., Choi, S. H., Hyman, B. T., & Tanzi, R. E. (2013). Alzheimer's disease risk gene CD33 inhibits microglial uptake of amyloid beta. *Neuron*, 78(4), 631–643.

Gu, L., & Guo, Z. (2013). Alzheimer's Aβ42 and Aβ40 peptides form interlaced amyloid fibrils. *Journal of Neurochemistry*, *126*(3), 305–311.

Hansen, D.V., Hanson, J. E., & Sheng, M. (2018). Microglia in Alzheimer's disease. *The Journal of Cell Biology*, 217(2), 459–472.

Hickman, S.E., Allison, E. K., & El Khoury, J. (2008). Microglial dysfunction and defective beta-amyloid clearance pathways in aging Alzheimer's disease mice. *The Journal of Neuroscience*, 28(33), 8354–8360.

Jiang, T., Yu, J.-T., Hu, N., Tan, M.-S., Zhu, X.-C., & Tan, L. (2014). CD33 in Alzheimer's Disease. *Molecular Neurobiology*, 49(1), 529–535.

Jonas, L. A., Jain, T., & Li, Y.-M. (2022). Functional insight into LOAD-associated microglial response genes. *Open Biology*, *12*(1), 210280–210280.

Kinney, J.W., Bemiller, S. M., Murtishaw, A. S., Leisgang, A. M., Salazar, A. M., & Lamb, B. T. (2018). Inflammation as a central mechanism in Alzheimer's disease. Alzheimer's & Dementia: *Translational Research & Clinical Interventions*, 4(1), 575–590.

Knopman D.S., Amieva H., Petersen R.C., Chételat G., Holtzman D.M., Hyman B.T., Nixon R.A., Jones D.T. (2021) Alzheimer disease. *Nature Reviews Disease Primers*, 7(1), 33.

Lajaunias F., Dayer J.M., Chizzolini C. (2005). Constitutive repressor activity of CD33 on human monocytes requires sialic acid recognition and phosphoinositide 3-kinase-mediated intracellular signaling. *European Journal of Immunology*, 35(1),243-51

Lopez, S., González, H. M., & Léger, G. C. (2019). Alzheimer's disease. *Handbook of Clinical Neurology*, 167, 231.

Lu, W., Gong, D., Bar-Sagi, D., & Cole, P. A. (2001). Site-Specific Incorporation of a Phosphotyrosine Mimetic Reveals a Role for Tyrosine Phosphorylation of SHP-2 in Cell Signaling. *Molecular Cell*, 8(4), 759–769.

Macklin, K. (2021). On the Frontlines of the Alzheimer's Crisis:: Advocacy Organizations in Delaware and Nationwide Urge Public Health Intervention to Curb Staggering Disease Trends. *Delaware Journal of Public Health*, 7(4), 20–23.

Miles, L. A., Hermans, S. J., Crespi, G. A. N., Gooi, J. H., Doughty, L., Nero, T. L., Markulić, J., Ebneth, A., Wroblowski, B., Oehlrich, D., Trabanco, A. A., Rives, M.-L., Royaux, I., Hancock, N. C., & Parker, M. W. (2019). Small Molecule Binding to Alzheimer Risk Factor CD33 Promotes Aβ Phagocytosis. *iScience*, *19*, 110–118.

Naj, A. C., Jun, G., Beecham, G. W., Wang, L. S., Vardarajan, B. N., Buros, J., Gallins, P. J., Buxbaum, J. D., Jarvik, G. P., Crane, P. K., Larson, E. B., Bird, T. D., Boeve, B. F., Graff-Radford, N. R., De Jager, P. L., Evans, D., Schneider, J. A., Carrasquillo, M. M., Ertekin-Taner, N., Younkin, S. G., …Schellenberg, G. D. (2011). Common variants at MS4A4/MS4A6E, CD2AP, CD33 and EPHA1 are associated with late-onset Alzheimer's disease. *Nature genetics*, 43(5), 436–441.

Patel, D. A., Henry, J. E., & Good, T. A. (2007). Attenuation of β-amyloid-induced toxicity by sialic-acid-conjugated dendrimers: Role of sialic acid attachment. *Brain Research*, 1161, 95–105.

Paul, S. P., Taylor, L. S., Stansbury, E. K., & Mcvicar, D. W. (2000). Myeloid specific human CD33 is an inhibitory receptor with differential ITIM function in recruiting the phosphatases SHP-1 and SHP-2. *Blood*, 96(2), 483–490.

Rabinovici, G. D. (2019). Late-onset Alzheimer Disease. *Continuum*, 25(1), 14–33.

Russo, D., Cappoli, N., Coletta, I., Mezzogori, D., Paciello, F., Pozzoli, G., Navarra, P., & Battaglia, A. (2018). The human microglial HMC3 cell line: where do we

stand? A systematic literature review. *Journal of Neuroinflammation*, 15(1), 259–259.

Schwab, C., Klegeris, A., & McGeer, P. L. (2010). Inflammation in transgenic mouse models of neurodegenerative disorders. *Biochimica et Biophysica Acta*, 1802(10), 889–902.

Shen, X-N., Niu, L.-D., Wang, Y.-J., Cao, X.-P., Liu, Q., Tan, L., Zhang, C., & Yu, J.-T. (2019). Inflammatory markers in Alzheimer's disease and mild cognitive impairment: a meta-analysis and systematic review of 170 studies. *Journal of Neurology, Neurosurgery & Psychiatry*, 90(5), 590–598.

Slatkin, M. (2008). Linkage disequilibrium - understanding the evolutionary past and mapping the medical future. *Nature Reviews Genetics*, 9(6), 477–485.

Stine, W. B., Jungbauer, L., Yu, C., & LaDu, M. J. (2011). Preparing Synthetic Aβ in Different Aggregation States. *Alzheimer's Disease and Frontotemporal Dementia*, 670, 13–32.

Taylor, V. C., Buckley, C. D., Douglas, M., Cody, A. J., Simmons, D. L., & Freeman, S. D. (1999). The Myeloid-specific Sialic Acid-binding Receptor, CD33, Associates with the Protein-tyrosine Phosphatases, SHP-1 and SHP-2. *The Journal of Biological Chemistry*, 274(17), 11505–11512.

Tam, V., Patel, N., Turcotte, M., Bosse, Y., Pare, G., & Meyre, D. (2019). Benefits and limitations of genome-wide association studies. *Nature Reviews Genetics*, 20(8), 467–484.

Wang, Tan, M.-S., Yu, J.-T., & Tan, L. (2015). Role of pro-inflammatory cytokines released from microglia in Alzheimer's disease. *Annals of Translational Medicine*, 3(10), 136–136.

Wardyn, J. D., Chan, A. S. Y., & Jeyasekharan, A. D. (2021). A Robust Protocol for CRISPR-Cas9 Gene Editing in Human Suspension Cell Lines. *Current Protocols*, 1(11), 286.

Weber, J., Peng, H., & Rader, C. (2017). From rabbit antibody repertoires to rabbit monoclonal antibodies. *Experimental & Molecular Medicine*, *49*(3), 305–305.

Wißfeld, J., Nozaki, I., Mathews, M., Raschka, T., Ebeling, C., Hornung, V., Brüstle, O., & Neumann, H. (2021). Deletion of Alzheimer's disease-associated CD33 results in an inflammatory human microglia phenotype. *Glia*, 69(6), 1393–1412.

Wißfeld, J., Mathews, M., Mossad, O., Picardi, P., Cinti, A., Redaelli, L., Pradier, L., Brüstle, O., & Neumann, H. (2021). Reporter cell assay for human CD33

validated by specific antibodies and human iPSC-derived microglia. *Scientific Reports*, 11(1).

Yamazaki, Zhao, N., Caulfield, T. R., Liu, C.-C., & Bu, G. (2019). Apolipoprotein E and Alzheimer disease: pathobiology and targeting strategies. *Nature Reviews. Neurology*, 15(9), 501–518.

Zhao, L. (2018). CD33 in Alzheimer's disease – biology, pathogenesis, and therapeutics: A mini-review. *Gerontology*, 65(4), 323–331.